Strål säkerhets myndigheten
Swedish Radiation Safety Authority

Authors: Georg A. Lindgren
Clifford Voss
Joel Geier

Research

# 2013:28

# Brine intrusion by upconing for a high-level nuclear waste repository at Forsmark

## Scoping calculations

Report number: 2013:28 ISSN: 2000-0456
Available at www.stralsakerhetsmyndigheten.se

## SSM perspective

### Background

SSM currently reviews a license application for a spent nuclear fuel repository that is proposed to be located at Forsmark, Sweden. The repository is to be situated at 500 m depth in the rock and copper canisters are deposited in holes excavated from the tunnel system. To protect the canisters they are surrounded by a bentonite clay buffer, which is to swell when getting in contact with water. The swelling properties are dependent on the salt content of the water and excessively high salt contents may inhibit the swelling. Thus it is important to ensure that the bentonite is not subjected to water with too high salt contents. The salt content of the groundwater increases with depth and is expected to reach levels that may affect buffer performance at large depths. When excavating the repository very high hydraulic gradients are established and water and salt movement from the depth to the repository, so-called 'upconing', could possibly occur.

### Objectives

The objective of this study is to evaluate the possibility of salt-water migration to the repository. This objective is motivated by the adverse impacts of water with too high salinity entering the repository and by the uncertainty of the relevant hydraulic and hydrogeochemical conditions at the Forsmark site at great depths. To analyse density dependent flow and salt transport at the Forsmark site the USGS' SUTRA code is used. This study proceeds by finding critical model cases for which upconing does or does not occur, while assessing whether the parameterizations of these cases are realistic for the Forsmark site. In addition, the fall of the upconed salt mound (i.e. downconing) following closure of the repository is also evaluated. In particular the objectives are (1) to determine the factors that control saltwater upconing in a hydrogeological setting representative of Forsmark; (2) to relate these factors to the plausible conditions prevailing at the repository site; (3) to investigate whether the proposed repository is likely to generate saltwater upconing, given the range of uncertainty in hydrogeologic structure and parameter values; and (4) to evaluate the timing of upconing (salinization) and the timing of downconing (freshening) following repository closure for cases where upconing occurs.

### Results

The results of this simulation analysis show that upconing behavior is strongly affected by the ratio of permeability to porosity in any zone in which upconing might occur. Within the full range of parameters that are likely to occur at the Forsmark site, the model yields either no significant upconing at all during the operational period of the repository or intrusion of brine-type waters after only one to a few decades.

### Need for further research

A relatively simple conceptual model like the one used in this study is helpful in defining the modes of upconing behavior that are possible, and in defining the factors controlling this process. More elaborate structural models could be used to check more carefully which of the range of conditions that are here found to be plausible for the Forsmark site are most applicable.

### Project information

Contact person SSM: Georg Lindgren
Reference: SSM 2010/2105

Strål
säkerhets
myndigheten
Swedish Radiation Safety Authority

**Authors:** Georg A. Lindgren[1)], Clifford Voss[2)] and Joel Geier[3)]
[1)]Swedish Radiation Safety Authority, [2)]US Geological Survey,
[3)]Clearwater Hardrock Consulting

# 2013:28

# Brine intrusion by upconing for a high-level nuclear waste repository at Forsmark

## Scoping calculations

**Date:** September 2013
**Report number:** 2013:28 **ISSN:** 2000-0456
Available at www.stralsakerhetsmyndigheten.se

This report concerns a study which has been conducted for the Swedish Radiation Safety Authority, SSM. The conclusions and viewpoints presented in the report are those of the author/authors and do not necessarily coincide with those of the SSM.

# Contents

# 1. Introduction

**BRINE INTRUSION AND REPOSITORY SAFETY -** In Sweden's proposed high-level repository located at Forsmark, Sweden (Figure 1), spent nuclear fuel is planned to be encapsulated in sealed cylindrical copper canisters (about 1 m diameter and 5 m high) and disposed of in cylindrical holes (about 1.80 m diameter and 7 m deep) at around 500 m below ground level in fractured crystalline rock. The repository is intended to contain and isolate the nuclear waste for over 100,000 years. The holes are to be excavated in the floors of a tunnel system in the rock (deposition tunnels 4.8 m high and 4.2 m wide) that extends from the ground surface to this depth (SKB, 2011). Due to very low groundwater flow within the repository host rock, the tunnel and deposition holes will remain relatively dry during excavation and canister emplacement (Svensson and Follin, 2010). The canisters are smaller than the deposition holes and within each deposition hole, the canister will be fully surrounded on all sides by a so-called 'buffer' composed of bentonite clay that swells when it absorbs water. When the canisters have been emplaced and surrounded by relatively dry but pure bentonite, the tunnel segments are closed off by backfilling with swelling Friedland clay. Then the backfilled tunnel and deposition holes slowly begin to resaturate with groundwater that flows in from the host rock. During resaturation, the swelling bentonite should fill all voids in the deposition holes between the canister and host rock, leading to a very dense barrier that allows only diffusive transport of solutes through the clay, protecting the canisters from corrodants within the groundwater and surrounding rock. This buffer also slows potential outward transport of leaking radionuclides, should any canister not be thoroughly sealed or somehow compromised at a later time.

However, salty water exists in the host rock and bentonite swelling is adversely impacted by the salt content of the water it absorbs (e.g. see Karnland et al., 2005); high salt content inhibits swelling. Thus, should salty groundwater enter some deposition holes and the tunnel during excavation and/or resaturation following repository closure, the resulting barrier may not meet the design requirements. Should the buffer not fully expand to fill the excavation voids as intended, its isolation function as one of the primary barriers within the repository's multi-barrier waste isolation system would be disturbed, adversely affecting the repository's ability to isolate nuclear waste, thereby decreasing safety margins. High salt content of the water flowing into the tunnel during excavation and emplacement may also be of concern for technical installations needed for the operation of the repository.

**BRINE EXISTENCE AND MIGRATION AT FORSMARK -** The salt content of groundwater in the fractured rock at the Forsmark site increases with depth (SKB, 2008). Based on extrapolating data from Forsmark and similar sites to greater depths, groundwater consisting of brine likely exists

at shallow-enough depths (around or less than 2000 m) such that upward migration of brine to a repository at 500 m depth could occur via driving forces described in the following.

When tunnels are excavated and exposed to the atmosphere, the water pressure at tunnel depth drops drastically from hydrostatic pressure of 50 atmospheres (5000 kPa) to atmospheric pressure (1 atmosphere or 100 kPa). This 50-fold decrease in pressure leads to a large hydraulic gradient in the groundwater around the excavation and thereby to an inflow of groundwater to the repository from all sides and an escape of air through the tunnel ventilation system. Relatively fresh groundwater (with low total dissolved solids content) will initially enter the repository through transmissive fractures from above and freshwater inflow will continue as long as there is a surface source of water, such as rainfall recharge, snowmelt or fresh surface-water bodies. Groundwater with low to intermediate ambient salinity may flow into the repository from the sides through transmissive fractures connected laterally to the repository. However, the focus of concern in this study is the potential for upward flow in a flow field that results from such a large pressure disturbance in a fluid distribution that generally exhibits increasing salt content and fluid density with greater depth. After repository excavation, the driving force for upward flow due to the low repository pressure is in opposition to the downward force due to buoyancy, in which denser salty water tends to sink. If the upward pressure force exceeds the downward buoyancy force, an upflow of relatively dense water with high salt content from depth may occur and may reach the repository. Such so-called saltwater upconing is a ubiquitous phenomenon in wells producing groundwater from coastal aquifers subject to seawater intrusion, having been widely-studied for purposes of water quality management, both experimentally and via numerical modelling (e.g. Reilly and Goodman, 1987; Prieto et al., 2006; Werner et al., 2009). Following repository closure, when the normal near-hydrostatic pressures are restored, ending the strong upward force, so-called downconing may occur, as any saltwater that has risen above the depth at which it is stable moves downward via buoyancy forces, which persist until the saltwater has reached its stable depth.

For the Forsmark site, Svensson and Follin (2010) calculated the influence of repository construction on groundwater flow and migration of saltwater using a 3-D finite volume continuum porous media model. The data underlying the model was taken from a detailed three-dimensional site-descriptive model of the Forsmark site (SKB, 2008). The transmissivity and porosity data used were based on a hydrogeological discrete-fracture network model of the area. The results for this particular description of the site indicated that upconing of water with high salinity during repository excavation would not occur. An earlier study by Svensson (2006) predicted small impacts of an open repository on the migration of saltwater, although uncertainties were

not elaborated. Despite these reported results, SKB (Swedish Nuclear Fuel and Waste Management Co), the organisation in Sweden tasked with developing Sweden's high-level nuclear waste repository, concluded at the end of the initial site investigation stage that one of the main hydrogeological uncertainties was the possibility for upconing of deep saline groundwater in steeply dipping rock deformation zones with relatively high transmissivity (SKB, 2008).

**THIS STUDY -** Motivated by the importance of the potentially adverse impacts of saltwater entering the repository and by the uncertainty of previous studies for the Forsmark site, this study evaluates the possibility of saltwater migration to the repository. To ensure that the excavation and emplacement phase of the repository can be managed in a safe manner, to ensure that the state of the repository prior to closure is well defined and well understood, and to ensure that the long-term safety of the repository will occur within planned margins (with particular regard to the performance of the bentonite buffer), it is important to develop understanding of potential inflow of saltwater into the tunnels in a more general manner than has been done previously, by considering a full range of possible structural configurations and hydrogeologic parameter values at the Forsmark site.

This study proceeds by finding critical model cases for which upconing does or does not occur, while assessing whether the parameterizations of these cases are realistic for the Forsmark site. In addition, the fall of the upconed salt mound (i.e. downconing) following closure of the repository is also evaluated. To accomplish generality, this study focuses on modeling two-dimensional (2-D) groundwater-flow and solute transport within a typical sub-vertical deformation zone that is parameterized based on site-specific data. The conceptual models are implemented in the U.S. Geological Survey's SUTRA finite-element code (Voss and Provost, 2002) that numerically calculates variable-density groundwater flow and advective-dispersive salt transport.

This groundwater simulation analysis thus has the following general objectives.

1- Determine the factors that control saltwater upconing in a hydrogeologic setting representative of Forsmark.

2- Relate these factors to the plausible conditions prevailing at the repository site.

3- Investigate whether the proposed repository is likely to generate saltwater upconing, given the range of uncertainty in hydrogeologic structure and parameter values.

4- For cases where upconing occurs, evaluate the timing of upconing (salinization) and the timing of downconing (freshening) following repository closure.

These results may then be employed to assess the possibility that saltwater will enter a Forsmark repository, and if so, for how long it may remain within the repository, so that possible adverse impacts on bentonite buffer swelling can be subsequently evaluated.

# 2. Methods

**CONCEPTUAL APPROACH -** Groundwater flow and salt transport in the fractured rock surrounding the planned Forsmark repository occurs primarily through a sparse set of structures consisting of intersecting vertical or sub-vertical and gently dipping fracture zones (deformation zones). Although some flow may pass laterally from one structure to another through the network of fractures in the rock domain, the primary impact of depressurization of repository tunnels is in the vertical direction, potentially resulting in upconing of saline water and downflow of shallow fresh water. Thus, vertical or sub-vertical zones that connect deep brine with the repository and the ground surface are the most important conduits for the process under consideration.

For the current analysis, the system is evaluated by simulating 2-D flow through sub-vertical deformation zones that transect the repository domain, defined as the area within the repository outline (Figure 1). Based on the repository outline proposed by SKB (SKB, 2009) the deformation Zone ENE0061 is chosen as a reference point for conceptualizing the problem (Figure 1) and the geometry of this zone is roughly used to define the geometry of the conceptual model. From this reference point, the analysis then explores a variety of cases based on data not solely related to the zone. In this way, a variety of deformation zones with differing hydrogeologic properties and differing external forcings that transect the repository domain are evaluated. Furthermore, the modeled cases specifically represent properties of Zone ENE0061 and Zone NNE0725 (for brevity, referred to herein as Zone 61 and Zone 725); these cases also cover a plausible range of property values for zones intersecting the Forsmark repository domain.

The model is conceptualized as a 2-D representation of a generic sub-vertical (i.e. nearly vertical) rock deformation zone that stretches from the ground surface down to the chosen bottom boundary of the model. The lateral length of the zone is taken from Figure 1 to be 2100m corresponding to the length of Zone 61. At its lateral ends, Zone 61 is intersected by other sub-vertical deformation zones. There are also several other sub-vertical zones intersecting Zone 61 (Figure 1). The deformation zone is also intersected by a large number of smaller fractures. It is assumed that the flow in the zone is substantially larger than the flow through the smaller fractures and these smaller fractures are therefore not explicitly represented in the model. This is in accordance with the conceptualization of the system used by SKB (SKB, 2008). SKB distinguishes between a hydraulic conductor domain, which ordinarily corresponds to a major deformation zone, and a hydraulic rock domain, which is made up of a discrete fracture network in the surrounding rock.

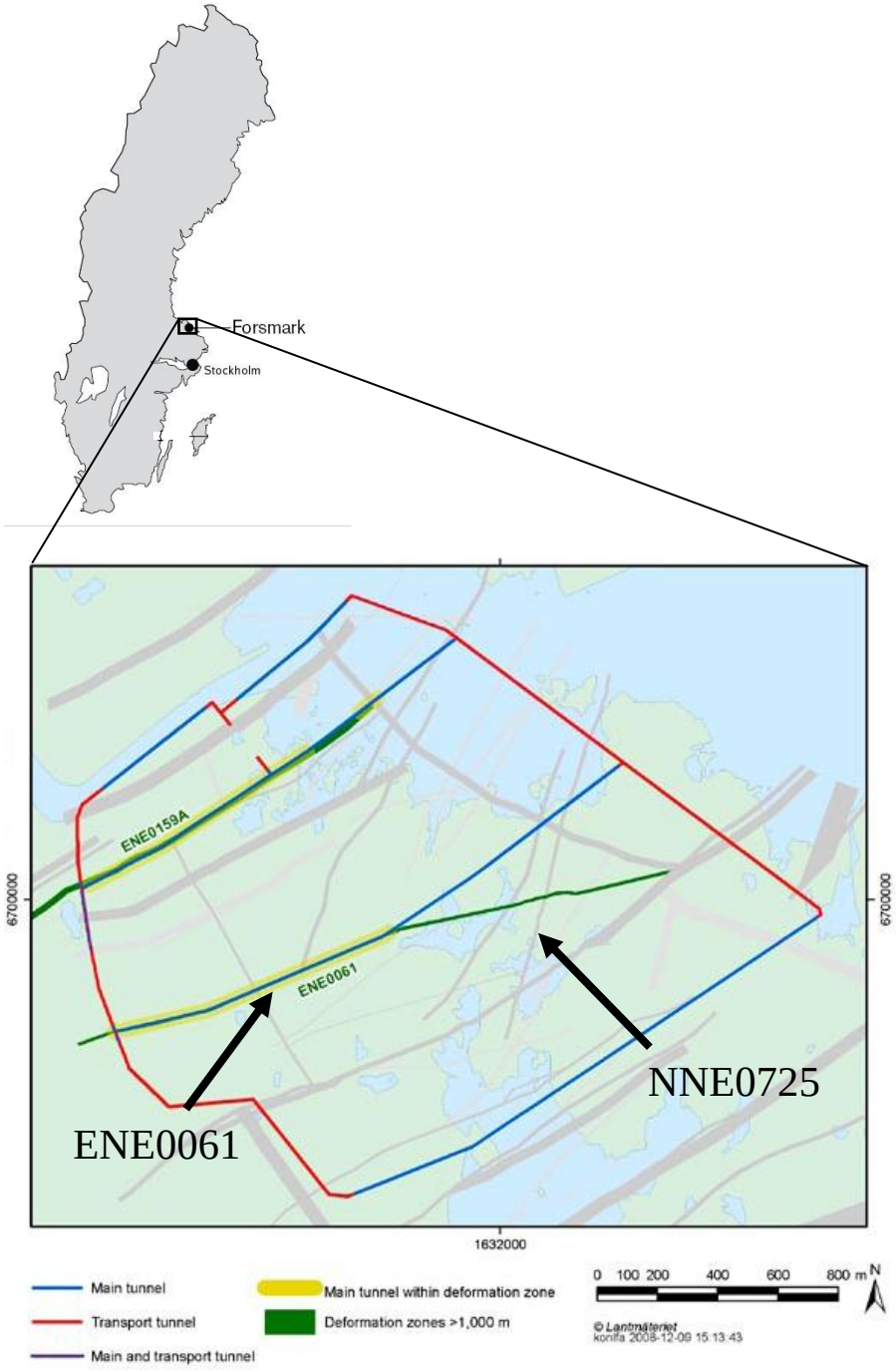


Figure 1. Map of Sweden indicating the location of Forsmark (above) and the layout of main and transport tunnels of the proposed repository at 470m depth at Forsmark (below). Zones ENE0061 and NNE0725 are indicated by arrows (modified from SKB, 2009, Fig 4-16). The regularly-spaced deposition tunnels with the waste canisters and bentonite buffer extend nearly perpendicularly to the main tunnels, with the appearance of teeth on a comb that nearly fill the repository domain outline that is delineated by the surrounding transport/main tunnels (see SKB, 2009, Fig 4-13 for details).

**NUMERICAL MODEL -** The numerical calculations of the various cases investigated in this study are carried out using the U.S. Geological Survey‘s SUTRA code (Voss and Provost, 2002). The SUTRA code can simulate fluid movement and the transport of salt in a subsurface environment. The code employs a 2-D or 3-D (three-dimensional) finite-element and finite-difference method to calculate numerical solutions to variable-density flow and solute transport problems.

# 3. Data

The full set of parameter values derived from SKB's site investigation data are used as a starting point for building the generalized models. Because the data and the assumptions used to derive the values are subject to some uncertainty, a Base Case model is set up to serve as a starting point for checking how changes in the assumptions and parameterization influence the upconing results. The ranges of the input parameters used in the model span the ranges observed at the Forsmark site.

**SALINITY -** The salinity of the water at the Forsmark site has been investigated by SKB (SKB, 2008) to a depth of almost 1000m. Figure 2 shows a compilation of salinity data (total dissolved solids) and least square linear depth-salinity fits for borehole data from Forsmark and Laxemar, Sweden, and Olkiluoto, Finland. Smellie et al. (2008) infer that drilling deeper than the available boreholes at the Swedish site investigation sites would intercept brines. In view of this assessment, SKB's salinity model results for Forsmark are here extrapolated to a depth where the salinity reaches brine levels (100g/L). This is found to occur at about 2100m depth, motivating use of a groundwater model domain reaching down to that depth. The extrapolation gives higher salinities at depths than the extrapolation of the KFM07a and KFM09a borehole salinity data, but lower values than the extrapolation of data from Laxemar, Sweden (deepest borehole KLX02) and Olkiluoto, Finland.

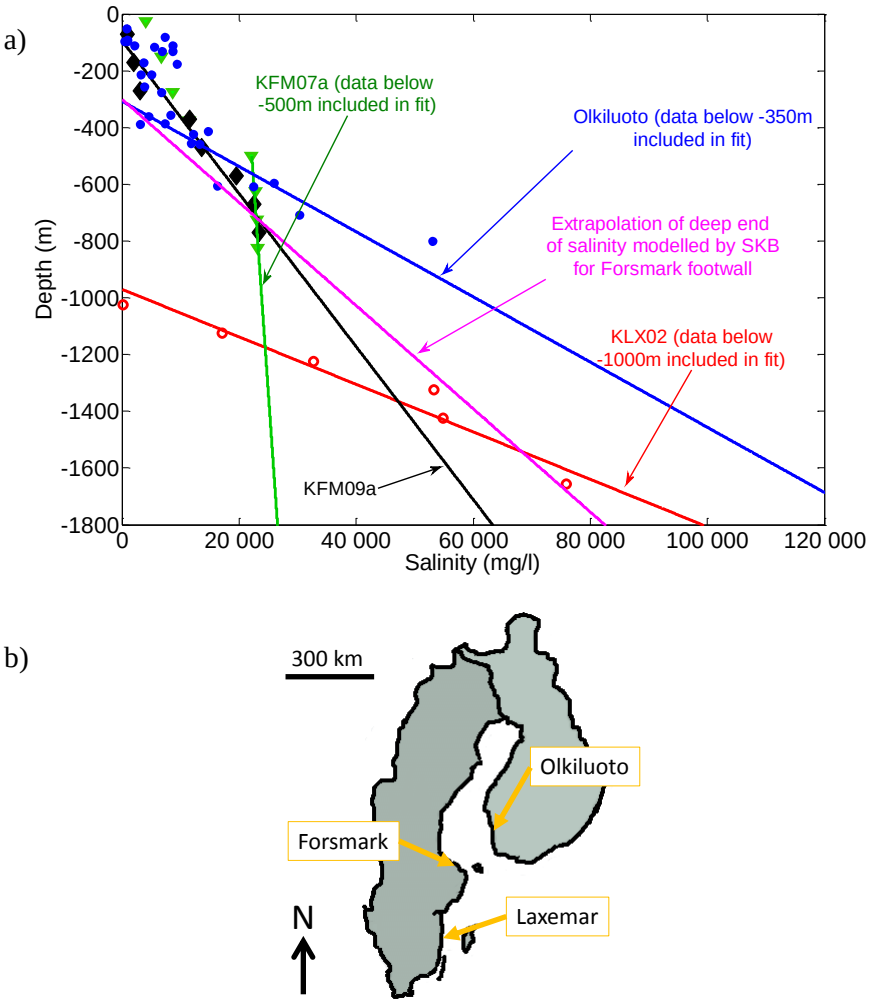


Figure 2: a) Compilation of selected salinity data (total dissolved solids) from Forsmark, Laxemar, and Olkiluoto together with linear extrapolations of the data to greater depths using a linear least squares fit. For Forsmark the two boreholes with the highest salinity values are shown (KFM07a, green triangles, Berg et al. (2005) p. 33; and KFM09a, black diamonds, Nilsson (2006) p.33). SKB's model for salinity against depth for the so called Forsmark footwall* below 500 m depth is extrapolated to larger depths than shown in their Figure (magenta line, SKB (2008), Figure 8-46 p. 276). Laxemar data show the deepest borehole KLX02 below 1000m (red open circles, Laaksoharju et al. (1999) p. 30; contributions from Mg, HCO3, Si, Li, Sr, and K are neglected). Olikiluoto data are from 2008 (blue filled circles, Pitkänen et al., 2009). Higher salinities than given in the 2008 dataset have been reported from Olkiluoto with a maximum of 84g/L (Pitkänen et al., 2009 p. 83 ). *Note: The footwall is defined as the body of rock that lies beneath the set of gently dipping deformation zones in the south of the investigated area.

b) Map showing location of salinity data measurements at sites within Sweden (left on the map) and Finland (right), all located along the coast of the Baltic Sea and Gulf of Bothnia.

**PERMEABILITY -** The transmissivity range of the modeled generic deformation zone is based on data from SKB's site investigation. Zones that connect the repository at about 500 m depth with possible brine at greater depths are the ones that might conduct brine to the repository and are thus the focus of this analysis. Two zones, one with relatively low transmissivity (Zone 61) and one with relatively high transmissivity (Zone 725) are chosen as reference parameterizations for the model (Table 1). Both zones intersect the repository tunnels and thus may contribute water inflow to the repository.

The transmissivity of Zone 61 is close to the lower limit of what can be measured and can thus be argued to be a lower limit for transmissivity. There are many zones with transmissivity below the measurement limit (Follin et al., 2007, e.g. Table 9-1), but these will host less saltwater upconing than zones with higher transmissivity, so can be neglected in this analysis. Considering a high transmissivity limit, Zone 725 is the most transmissive that crosses the repository domain (based on information in Follin et al, 2007, and Stephens, 2007). There is one zone with higher measured transmissivity at relevant depth outside the repository domain, but this will not impact upconing in the repository domain. There are no transmissivity data for depths greater than 900 m and because connections to brines at depths of as much as 2100 m must be considered, the transmissivity at these depths must be extrapolated from shallower data.

There are many gently dipping zones with transmissivity greater than Zone 725 (Follin et al., 2007, max $1.2 \times 10^{-3}$ $m^2/s$ at 130 m depth, i.e. almost 4 orders of magnitude greater than Zone 725), but these lie above and partly outside the repository domain. There is one measured zone at about 430 m with transmissivity of $1.2 \text{x-} 10^{-6}$ $m^2/s$, half an order of magnitude greater than Zone 725 and also at a relevant depth. However this zone lies at the border of the repository domain and will not directly impact the repository. There are also structures at depths less than 300 m that are more transmissive (maximum about 2 orders of magnitude greater than Zone 725 at 200 m depth). However (as will be clear from the results presented later in this analysis), the transmissivity of structures below the repository, not above, exert the greatest control on upconing behaviour, so the shallow high transmissivity structures are not as important in the current analysis.

Because variable-density flow is simulated, the SUTRA model requires permeability values and so the transmissivities derived from SKB's measurements need to be expressed as permeabilities. To accomplish this, hydraulic conductivity values are first calculated from the transmissivities, requiring definition of zone thicknesses, which are based on data from the boreholes that intersect the zones. Zone 61 is intersected by borehole KFM01d and KFM06a and Zone 725 is intersected by borehole KFM 06a (SKB, 2007). In Table 1, all the data required for calculating the permeabil-

ity of the zones from available measurements are given, together with the respective references. For all modelled cases except the spatial trend and heterogeneity cases the permeability is assumed to be constant throughout the model domain. When there are measurements of the transmissivity from several measurement sections in the borehole interval in which the deformation zone is located, the transmissivity values are summed to get the total transmissivity of the zone. The hydraulic conductivity is then calculated by dividing the transmissivity by the zone thickness. For Zone 61, the geometric mean of the conductivity values from the injection test measurements in the two borehole intersections is used to calculate the effective conductivity of the zone. This is based on the fact that, assuming 2-D steady flow in an unbounded isotropic lognormal conductivity field, the effective conductivity can be calculated by taking the geometric mean of the measured values (e.g. Rubin, 2003). The permeability k is then obtained from the conductivity using $k = \frac{K \cdot \mu}{\rho \cdot g} \approx K \cdot 10^{-7}$ms with K being the hydraulic conductivity (m/s), $\mu$ the dynamic viscosity, $\rho$ the density of water and g the gravitational acceleration. For Zone 61, this yields a permeability of $6.7 \times 10^{-18}$ $m^2$ and for Zone 725, $1.8 \times 10^{-15}$ $m^2$ (using the geometric mean of the measurements with the two methods). (The available 'difference flow meter' measurements are not used for Zone 61, since they are close to the measurement threshold (Hjerne et al., 2005, Väisäsvaara et al., 2006) and the injection test results are considered more trustworthy).

**POROSITY -** To calculate transport of dissolved salt, the effective porosity values of the deformation zones are required. For all modelled cases except for some spatial trend cases the porosity is assumed to be constant throughout the model domain. The effective porosity value $9 \times 10^{-4}$ is used for representing Zone 61. This number is obtained by dividing the sum of apertures in the interval (calculated by summing the apertures described in Pettersson et al. (2005)) by the length of the borehole interval. Both 0.028 m/30 m and 0.02 m/20 m yield approximately a porosity of $9 \times 10^{-4}$. For Zone 725, similar reasoning yields a porosity of (0.05 m)/(35 m) = $1.4 \times 10^{-3}$. This calculation assumes that all fractures with an aperture in the interval that the zone intersects are parallel to the zone and participate in carrying active groundwater flow. Since many of the indicated apertures are close to the resolution of the method, these were assigned 0.5 mm (Pettersson et al., 2005 and 2006). The actual porosity of the zone at the borehole intersection may thus differ from these calculated estimates. This and the very likely spatial variability of the porosity within the zone make a sensitivity analysis necessary for a range of porosity values.

**Table 1: Summary of data for calculation of permeability and porosity for Zones 61 and 725. Hydraulic conductivity values are calculated by dividing transmissivity by zone thickness. References are listed below the Table.**

| Borehole | Borehole interval (m) | Zone thickness (m) | Sum of apertures (mm) | Injection test transm. ($m^2/s$) | Injection test hydraulic conductivity (m/s, calculated) | Difference flowmeter transm. ($m^2/s$) | Difference flowmeter hydraulic conductivity (m/s, calculated) |
|---|---|---|---|---|---|---|---|
| Zone ENE0061 | | | | | | | |
| KFM01D | 670-700[(1)] | 11[(1)] | 28[(2)] | $1.38 \times 10^{-9}$[(3)] (sum) | $1.25 \times 10^{-10}$ | Below threshold[(4)] | - |
| KFM06A | 788-810[(1)] | 11[(1)] | 20[(5)] | $4.00 \times 10^{-10}$[(6)] | $3.64 \times 10^{-11}$ | $3.70 \times 10^{-9}$[(6)] | $3.36 \times 10^{-10}$ |
| Zone 725 | | | | | | | |
| KFM06A | 740-775[(1)] | 12[(1)] | 50[(5)] | $1.37 \times 10^{-7}$[(6)] (sum) | $1.14 \times 10^{-8}$ | $3.57 \times 10^{-7}$[(6)] (sum) | $2.98 \times 10^{-8}$ |

[(1)] SKB R-07-45, p. A15-72 ff. and 96 ff. (Stephens et al., 2007)
[(2)] SKB P-06-132, Appendix 1 (Boremap log; Pettersson et al., 2006)
[(3)] SKB P-06-195, Table 6-2, p. 32 (Florberger et al., 2006)
[(4)] SKB P-06-161, Appendix 5, p. 100 (Väisäsvaara et al., 2006)
[(5)] SKB P-05-101, Appendix 1 (Boremap log; Pettersson et al., 2005)
[(6)] SKB P-05-165, Table 6-4, p. 64 (Hjerne et al., 2005)
See also SKB P-07-127 p. 28 and SKB P-06-56 p. 22 for correlation of Posiva flow log and boremap data for KFM01d (Teurneau et al., 2008) and for KFM06a (Forssman et al., 2006), respectively.

**GROUTING -** Zone 61 influences the proposed layout of the repository (Figure 1, blue main tunnel overlaps the zone) due to a transport tunnel that is to be excavated along a part of the zone. This tunnel will be grouted if necessary. Three levels of grouting efficiency give three values of residual transmissivity after grouting (Svensson and Follin, 2010). The conductivity data calculated for Zone 61 (Table 1) show lower conductivity values than the most stringent grouting level in Table 4-3 (p. 43) in SKB R-09-19 (Svensson and Follin, 2010), i.e. between $1 \times 10^{-8}$ m/s and $1 \times 10^{-9}$ m/s depending on the hydraulic conductivity before grouting. The modeled conductivity of the zones ranges from $1 \times 10^{-11}$ m/s to about $2 \times 10^{-8}$ m/s. Because the assumed range of permeability already includes the range possible after grouting, effects of grouting are not separately evaluated in this model analysis.

# 4. Model construction

**MODEL DOMAIN -** The 2-D model constructed (Figure 3) is 2100 m wide and 2000 m deep and is assigned a typical thickness of 11m representing the width of Zone 61 (Table 1) (and approximately representing the 12 m width of Zone 725). The repository is 1700 m wide and is modeled as 6 m high and for simplicity 11 m wide (main tunnels are planned to be 10 m wide, deposition tunnels 4.2 m wide; SKB 2009), and is located at 500 m depth within the model domain. The repository is represented by a hole in the model mesh, making it possible to separately calculate inflow of water and salt into the repository from above and below with SUTRA. The depth of the model bottom is set to the location at which salinity is assumed to be 100g/L. This is the depth from which brine, which may be problematic for repository operation, may derive.

**DISCRETIZATION AND BOUNDARY CONDITIONS -** The model domain is divided into 105 finite elements in the horizontal direction, yielding an element spacing of 20 m. In the vertical direction, the domain is divided into 25 elements above the repository and 75 elements below the repository with an element spacing of about 20 m. At the depth of the repository, the domain is divided into two layers of elements of size 3 m in the vertical direction, giving a total repository height of 6 m. The mesh refinement at repository depth allows the repository top and bottom to be represented by one row of nodes each. The repository is represented by a hole in the mesh with specified pressure boundary conditions around the perimeter of the hole. The total repository length is 1700 and the ends of the repository are 200 m from the nearest fracture zones that transect the modeled zone. In total, the finite-element mesh consists of 10540 elements and 10834 nodes (Figure 3). The effect of changing the spatial and temporal resolution of the model on the results was checked with the result that the chosen resolution gives acceptable results that do not significantly change by increasing the temporal or spatial resolution.

To simplify representations of the repository for downconing calculations, the repository volume after closure of the whole repository or part is not represented as a hole surrounded by specified pressures, but rather as a contiguous region of finite elements containing specified pressure nodes wherever the repository is still open (with pressure set equal to zero, i.e. atmospheric pressure). For the portions of the repository that are closed, no pressures are specified as a boundary condition and the pressure is calculated in the normal way by the model assuming that the closed back-filled repository has the same permeability as the surrounding bedrock.

The boundary conditions for pressure and salinity for the Base Case are shown in Table 2. In this analysis, several critical cases are considered in order to test the influence of different boundary conditions on the predicted flow fields.

**INITIAL CONDITIONS -** Initially, meaning, before excavation of the repository in the model simulations, the salinity is defined to be zero at the top boundary, linearly increasing to 23 g/L at 800 m depth in the model, which is the deepest measured value at the Forsmark site. From 800 m depth to the bottom boundary at 2000 m depth, the initial salinity then increases linearly from 23 g/L to 100 g/L. The value at the bottom boundary approximately agrees with the extrapolation of SKB's modeled salinity values for the Forsmark footwall (SKB, 2008; Figure 8-46 p. 276, see also Figure 2).

**Table 2: Boundary conditions for the Base Case defining pressure and the salinity of water flowing into the model.**

| Boundary | Pressure | Salinity of inflowing water where pressure is specified |
|---|---|---|
| Top | 0 | 0 |
| Bottom | Hydrostatic pressure value accounting for initial salinity increase with depth | 100 g/L |
| Left | Hydrostatic pressure value accounting for initial salinity increase with depth: $-9810 \cdot y - 0.098713125 \cdot y^2; \quad y \geq -800m$ $-9615.435 \cdot y + 0.22031625 \cdot y^2 - 48526.8; \quad y < -800m$ | Corresponding to initial salinity distribution: $-2.875 \cdot 10^{-5} y; \quad y \geq -800m$ $-0.028333333 - 6.41667 \cdot 10^{-5} y; \quad y < -800m$ |
| Right | Hydrostatic accounting for salinity increase with depth, see above | Corresponding to initial salinity distribution, see above |
| Repository | 0 | 0 |

a)

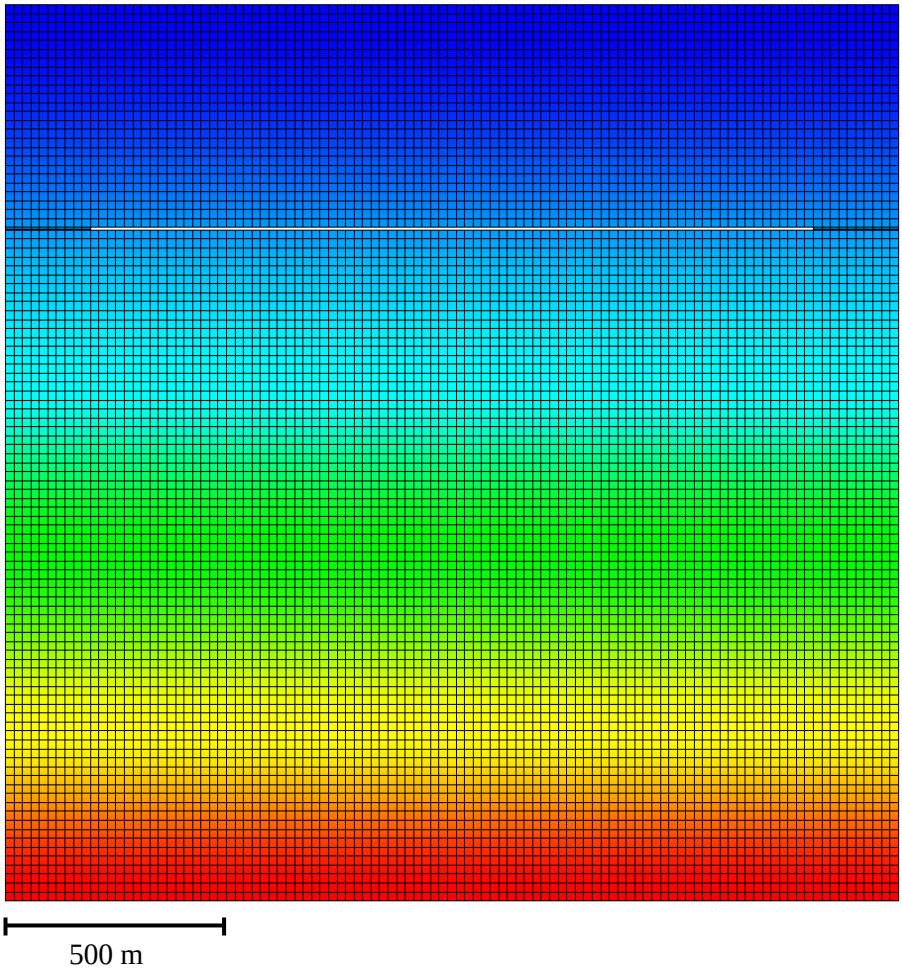


b)

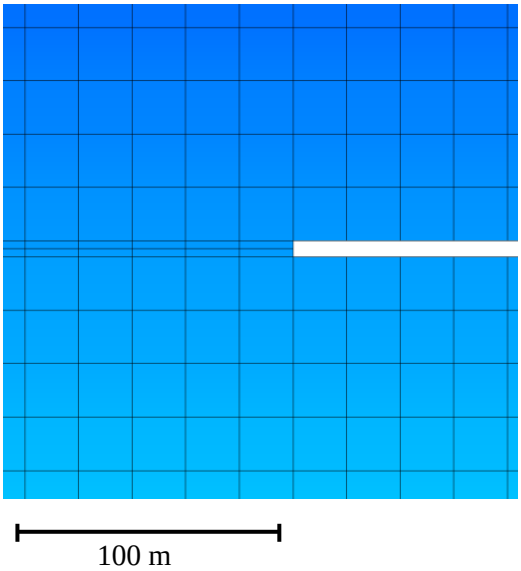

c)

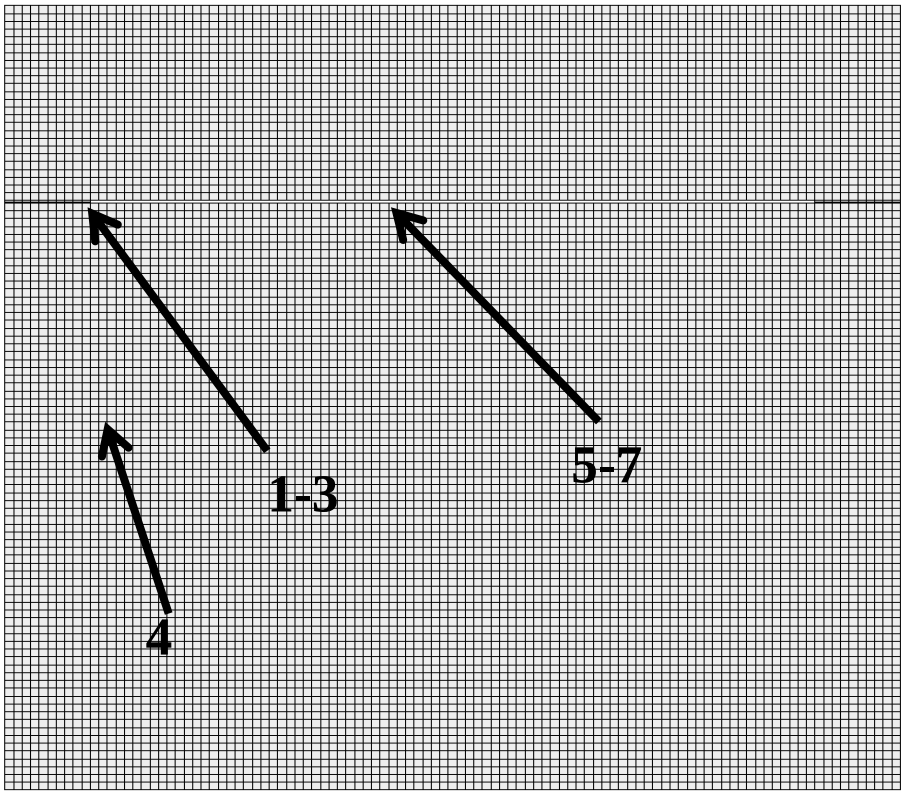


Figure 3: a) Model domain and mesh (2100 m x 2000 m) showing the repository as a hole in the mesh at 500 m depth. The color shows the initial salinity distribution increasing from zero at the top to 10% (100 g/L) at the bottom. b) A detail of the mesh around 500 m depth shows discretization near the left end of the repository. The size of the large cells is about 20 m x 20 m. c) Model domain and mesh showing the location of observation points used for recording time series of modeling results.

**MODEL OUTPUT -** Several observation points are located within the model domain (Table 3, Figure 3c) to record details of the temporal evolution of the simulated salinity as model output, in addition to the maps of flow and salinity produced at selected times for the entire model domain. The Base Case simulation is carried out with a temporal resolution (i.e. time step) of one year for a time period of 200 years. The modelling results are recorded every 10 years for the entire domain. Observations at the seven observation points (Table 3) are recorded every year.

**OTHER PARAMETERS -** All other parameters needed for running the model are listed in Table 4. Dispersivity values are for the Base Case model only; all other values are fixed for all simulations.

**Table 3: Position of observation points. Location of the observation points in the model domain. The coordinate system has its origin (x=0, y=0) at the upper left corner of the mesh, with x increasing to the right and y upwards (Figure 3c).**

| Observation point | x (m) | y (m) |
|---|---|---|
| 1 | 200 | -497 |
| 2 | 200 | -500 |
| 3 | 200 | -503 |
| 4 | 200 | -1002 |
| 5 | 1040 | -497 |
| 6 | 1040 | -503 |
| 7 | 1040 | -563 |

**Table 4: Additional model parameters.**

| | |
|---|---|
| Longitudinal dispersivity | 5 m |
| Transverse dispersivity | 0.1 m |
| Fluid compressibility | 4.47e-10 kg/(m $s^2$) |
| Apparent diffusivity (diffusion coefficient) of solute in fluid | 1.x$10^{-9}$ $m^2$/s |
| Density of water ($\rho_0$) | 1000 kg/$m^3$ |
| Fluid viscosity | 0.001 kg/(m s) |
| Solid matrix compressibility | 1.x$10^{-8}$ kg/(m $s^2$) |
| Density of solid rock | 2600 kg/$m^3$ |
| Acceleration of gravity | 9.81 m/$s^2$ |
| Fluid coefficient of density change with concentration | 700 |
| Density function for saline water | $\rho = \rho_0 + 700(C - 1000\frac{kg}{m^3})$ |

# 5. Analysis

To study the impact of repository excavation and closure on the distribution of groundwater salinity, a sequence of events is considered in a series of simulations. Initially, there is a natural salinity distribution that is represented in the model as an initial condition with the corresponding initial pressure condition that consists of a natural steady-state pressure distribution in agreement with both initial salinity and model boundary conditions.

For the main sequence of simulations, at time zero, the entire repository is instantaneously opened, dropping pressures along repository walls, which were initially at high values, to zero. This initiates both downflow of groundwater from above, upflow of groundwater from below, and lateral inflow from intersecting fracture zones on the sides, as though groundwater were moving towards a horizontal pumping well. Simulation results for salt distributions that result from the flow field generated by the repository are displayed below for particular elapsed times after repository opening, up to a time of 200 years after excavation. In some cases, the flow field and salt transport are also simulated for a period of time after repository closing in order to evaluate downconing behavior. Phased excavation and closing is considered in a separate case.

The model was run through this sequence for the Base Case parameterization presented above and also for a variety of other cases, in order to explore the effect of changing various parameters and boundary conditions, in light of the uncertainty in knowledge of actual system properties. The range of parameter values and conditions considered are expected to cover the full plausible range of possibilities for the site, such that true upconing behavior should be represented by one of the combinations considered, given the conceptual uncertainties of the model.

## 5.1 Base case

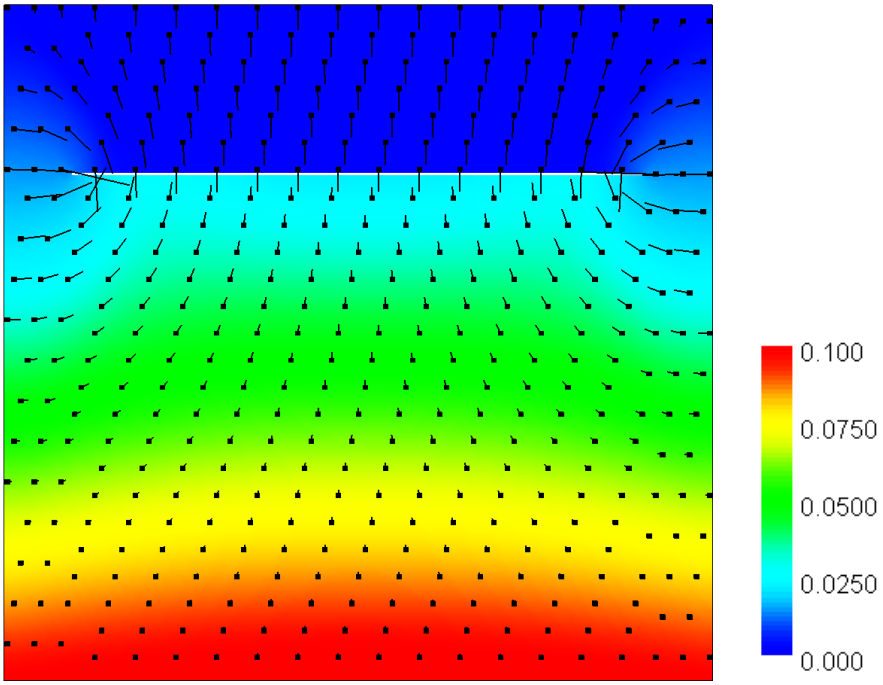


Figure 4: Salinity at time 200 years after excavation of repository for the Base Case, (with Zone 61 permeability). Colors indicate mass fraction of salt, i.e. 0.1 represents 10% salt in the water by weight. The velocity vector length is proportional to fluid velocity magnitude and flow direction directed along line away from square base of vector. The longest vector in the plot corresponds to a water velocity of $5x10^{-7}$ m/s.

Results for the Base Case parameterization representing the permeability of Zone 61 are shown in Figure 4. There is very limited movement of salt to the repository. Salinity is still slowly increasing even after 200 years of a completely open repository and the salt content has increased from about 1.5% to only about 2.1% at the repository center, where it is greatest. At the sides of the repository, the salt content of the inflowing water has hardly changed at all, remaining at 1.5% (from 1.45% to 1.52%). In contrast, Figure 5 (lower panel) shows a breakthrough of water with a salt content that reaches steady-state after only 25 years, with the rather high salinity of 10%, for the case representing the permeability for Zone 725.

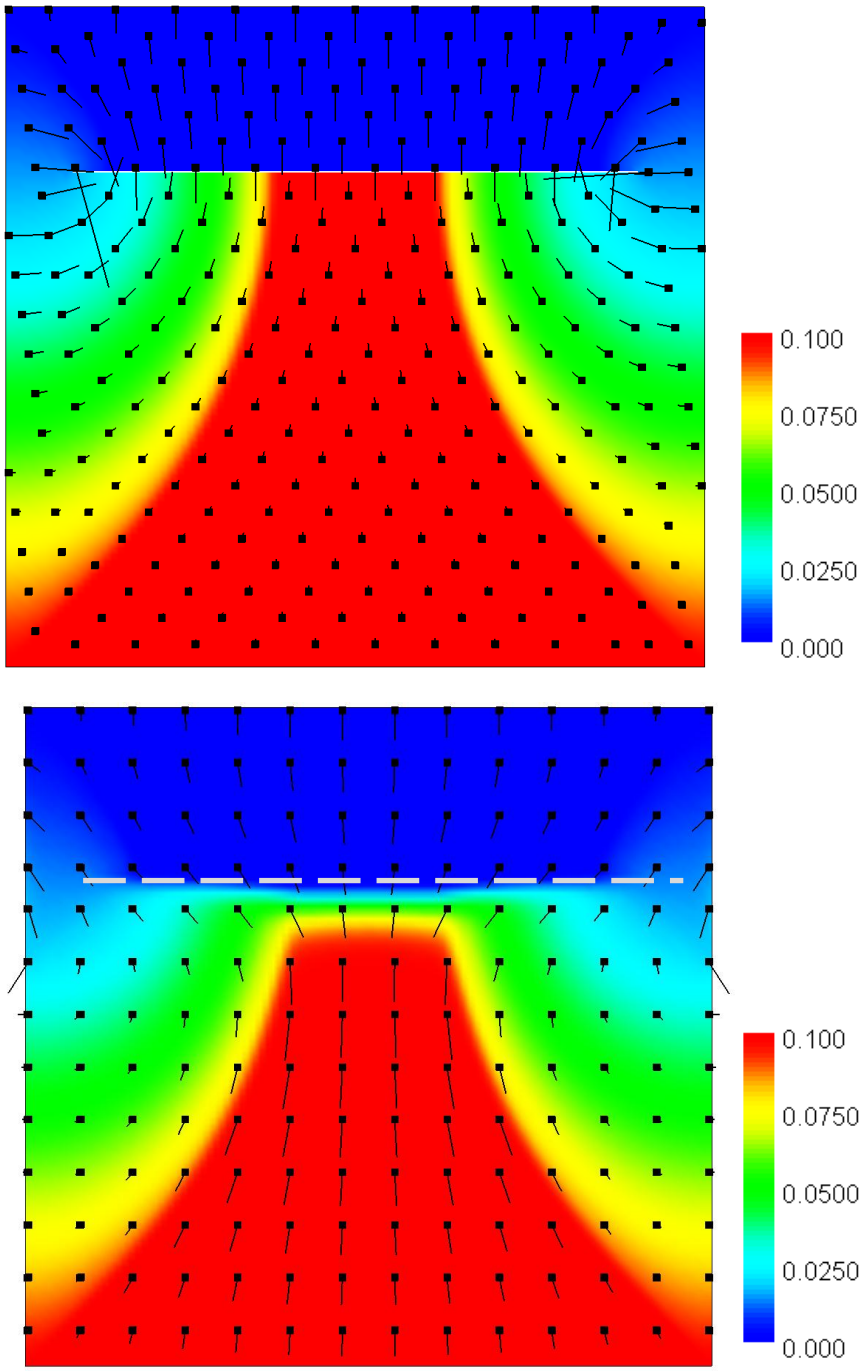


Figure 5: Salinity at time 25 years after excavation of repository (above), for the Base Case (with Zone 725 permeability) showing upconing. Salinity at time 10 years after closure of the repository (below), showing downconing. The dashed line indicates the location of the closed repository. Colors indicate mass fraction of salt, i.e. 0.1 represents 10% salt in the water by weight. The velocity vector length is proportional to fluid velocity magnitude and flow direction directed along line away from square base of vector. The longest velocity vectors for the upconing and downconing case correspond to 8 x $10^{-5}$ m/s and 5 x $10^{-7}$ m/s for the upconing and downconing case, respectively.

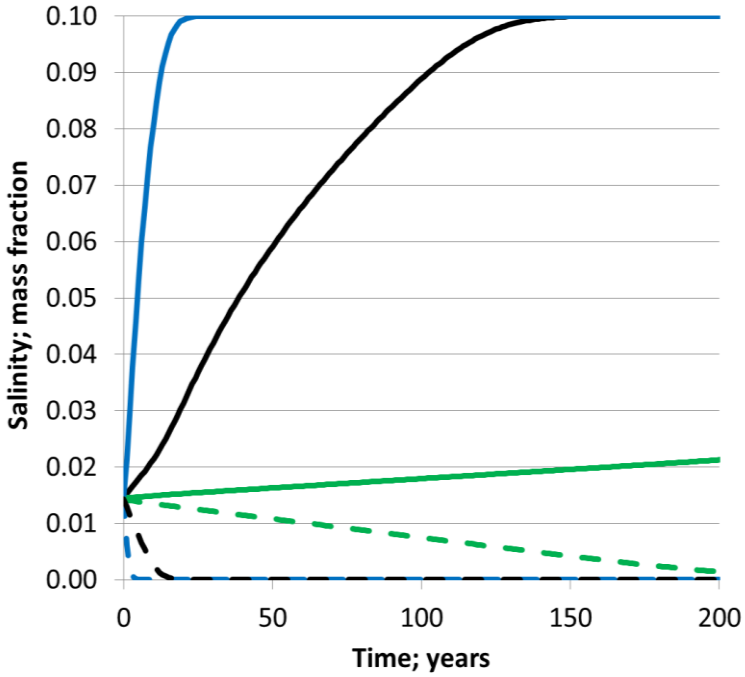


Figure 6: Breakthrough curves for the Base Case for observation point 6 (Figure 3c) in the mid-bottom of the repository (full lines) and observation point 5 in the mid-top of the repository (dashed lines). Breakthrough shown for permeability of Zone 61 ($6.7x10^{-18}m^2$; green lines), Zone 725 ($1.8x10^{-15}m^2$; blue lines) and for a case with intermediate permeability ($1.3x10^{-16}$ $m^2$; black lines).

As occurs for Zone 61, the salinity at the ends of the repository for the case of permeability representing zone 725 is also nearly unchanged. This is expected since the repository draws the water from the closest boundary, and the boundary condition concentration at repository depth has been set equal to the initial condition at the repository. Breakthrough curves for points above and below the repository center for the permeability cases shown in Figure 5, as well as for an intermediate permeability of $1.3x10^{-16}$ $m^2$, are shown in Figure 6.

The simulated influx of water to the repository from the zone amounts to 0.2 $m^3$/day for the low-permeability zone and 45.7 $m^3$/day for the high-permeability zone after 200 years. The simulated amount of salt entering the repository is 2 kg/day and 930 kg/day, respectively, at time 200 years. For Zone 725, the amounts at 25 years and at 200 years are equal because a steady state is already reached at 25 years. For both cases, about 60% of total inflow occurs to the top of the repository and about 40 % occurs along the floor of the repository.

The post-closure downconing for the Zone 725 case (Figure 5, upper panel) occurs relatively quickly. By 10 years following closure, the cone has sunken over 100 m (Figure 5-upper panel) and it continues to sink further. It can be noted that the water at the closed repository is fresher during downconing than it was under the initial conditions, because the sinking body of previously-upconed saltwater causes a downflow of freshwater from the top surface of the model (Figure 5).

## 5.2 Effect of topography and different boundary conditions

In these variations, the impacts of topography and differing lateral and bottom boundary conditions on upconing are investigated. Topographic undulation and trend in surface hydraulic head are neglected in the Base Case wherein a constant pressure of zero is assigned at the top boundary, representing a flat water table. A case was run explicitly considering the topography as a tilted sinusoidally-undulating surface with the mean height varying 10 m across the domain, a wavelength of 300 m, and with peak-to-peak amplitude of 6 m. For freshwater calculations without a repository, this yields a flow field with very low groundwater velocities, due to the low transmissivity of the modeled structure and the small gradients. (A higher transmissivity of the soil and uppermost rock is not accounted for in the model because this is not expected to significantly impact the flows being studied at depth.) The simulation with topography present and with initial salinity as in the Base Case displays no observable influence of the topography on the flow field compared to the case without the topographic variation (result not shown).

The Base Case has specified hydrostatic pressures at the left, right and bottom boundaries that are in equilibrium with the initial saltwater distribution. This represents the situation in which water from transecting structures can laterally enter/exit the studied sub-vertical structure. A variant simulation was also run with closed vertical subsurface boundaries, i.e. with no flow boundaries along left and right sides, representing the case where no lateral flow occurs from/to transecting structures. Another variant simulation was run with hydrostatic conditions that were specified for the Base Case at the left and right boundaries, but with a no-flow boundary at the bottom. The latter case represents the situation in which the bottom of the studied structure is closed to flow and all flow enters/exits from transecting structures. Salinities and breakthrough curves for these simulations are shown in Figure 7 and Figure 8.

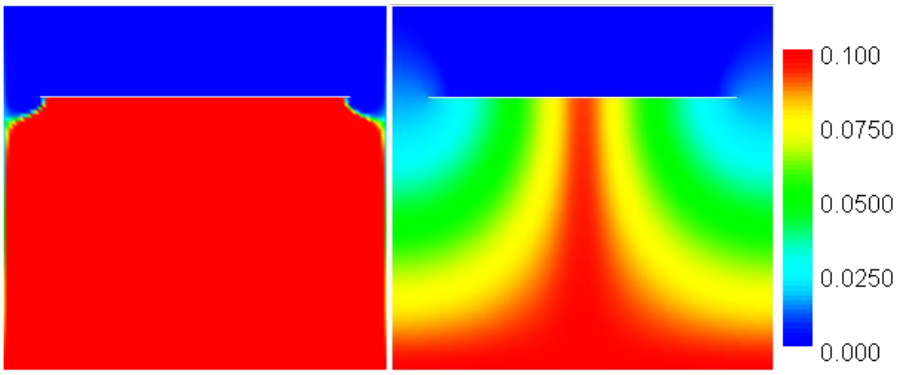


Figure 7: Salinity at steady state for no flow boundaries at the sides (left) and closed bottom boundary (right). Colors indicate mass fraction of salt, i.e. 0.1 represents 10% salt in the water by weight.

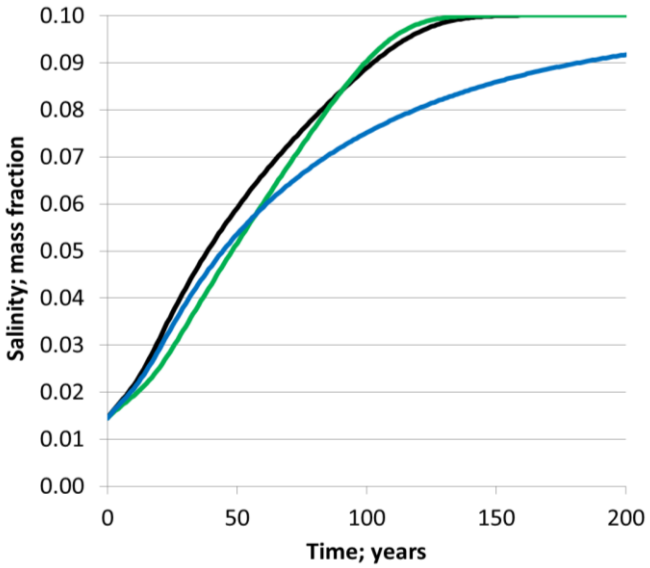


Figure 8: Breakthrough curves for different boundary conditions for observation point 6 in the mid-bottom of the repository using the intermediate permeability value shown in Figure 6. Hydrostatic subsurface boundaries (black line – Base Case), no flow lateral boundaries (green line), and no flow bottom and hydrostatic lateral boundaries (blue line).

The amount of water entering the repository is rather similar for the three cases, with the closed lateral case being about 30% lower and the case with the closed bottom about 2%. Compared to the Base Case, the salt mass in-flow rate for the closed lateral case is about 25% lower and for the case with the closed bottom is about 17% lower. There is a large salt intrusion for the case of closed lateral boundaries with high concentration throughout the repository (Figure 7 left panel). However, it should be noted that although all fluid in the rock below the repository becomes highly salinized, salt influx to

the repository is actually smaller than for the Base Case and the case with closed bottom, because the water inflow to the repository from below is lower than for these cases.

For closed side boundaries, there is more widespread intrusion of high salinity to the repository at steady state for all fracture zone permeabilities. The evolutions of salinity at the repository center are similar for the Base Case with all open boundaries and the case with closed side boundaries (compare in Figure 8), but the spatial distributions are different with more widespread upconing in the closed boundary case (compare Figure 5- lower panel with Figure 7-left panel). For a closed bottom boundary, the amount of intrusion is decreased relative to the Base Case, noting that the upconed area in Figure 7-right panel is narrower than in Figure 5- lower panel. In fact, the upconed area decreases with higher permeability when the bottom boundary is closed (simulation results not shown), providing the possibility of a situation wherein there is no significant upconing from directly below the repository, although zone transmissivity is high.

## 5.3 Effect of initial salinity distribution

As there is only limited information on the current distribution of subsurface salinity at the Forsmark site, four initial salinity distributions were tested to explore their effect on possible upconing and downconing behavior. These simulations were run with a permeability of $1.3x10^{-16}$ $m^2$, a value between the values for zone 61 and 725. In the first simulation, the initial salinity is modeled as specified above for the Base Case, i.e. linear increase from zero to 2.3% from the ground surface to 800 m depth and then linear increase to 10% at 2000 m depth. In a second simulation the increase to 800 m depth is the same but the value is then held constant at 2.3% down to 2000 m. The salinity of water flowing into the domain at the bottom is still set to 10%. In the third case, the initial salinity distribution is the same as for the other cases down to 800 m and then it linearly increases to 7.5% at 2000 m depth. In the fourth case, the same initial salinity distribution is applied down to 800 m and then the salinity increases linearly to 10% at 1500 m depth. Below 1500 m the salinity is constant at 10%.

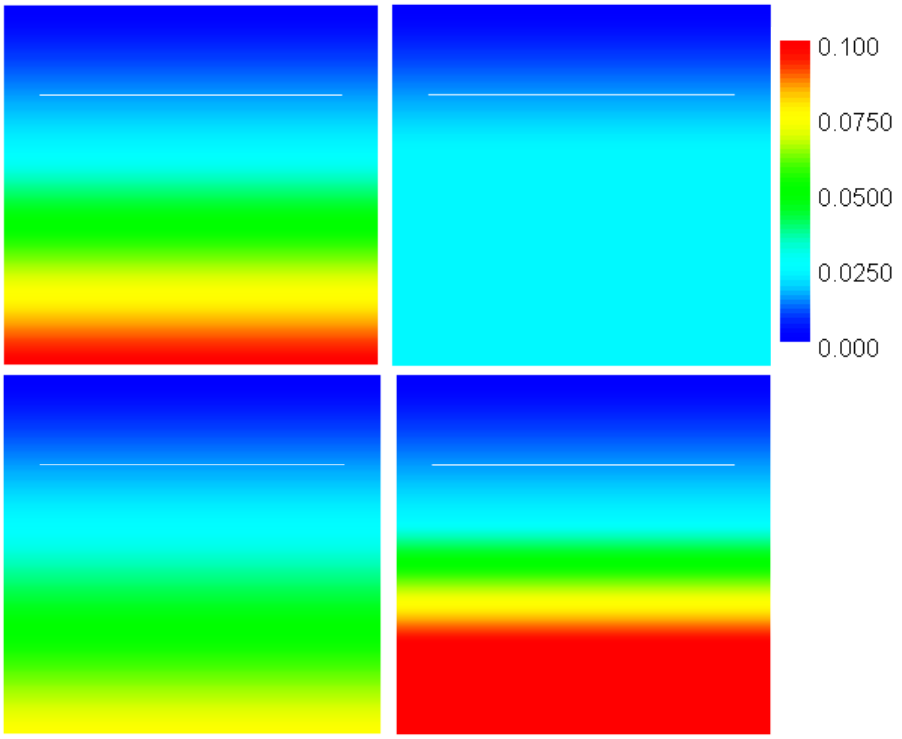


Figure 9: Initial salinity distributions for checking the effect of the initial salinity distribution. The left upper panel shows the salinity distribution linearly increasing from zero to 2.3% from the ground surface to 800 m depth (deepest measurement at Forsmark) and then linearly increasing to 10% at 2000 m depth, corresponding to Figure 3. In the upper right panel the increase to 800 m depth is the same but the value is then held constant at 2.3% down to 2000 m. The lower left panel shows an initial salinity distribution as for the other down to 800m and then linearly increasing to 7.5%. The lower right panel shows the same salinity distribution down to 800m and the linearly increasing to 10% at 1500 m depth. Below 1500 m the salinity is constant at 10%. Colors indicate mass fraction of salt, i.e. 0.1 represents 10% salt in the water by weight.

Results show that a situation with brine entering the repository, as shown in Figure 5 (lower panel), is reached after about 145 years for the case with the salinity increasing to the bottom of the domain. In the case with constant salinity below 800 m, the salinity in the water entering the repository increases for about 15 years from 1.6% to 2.3% and then is constant at this value until about 65 years when the salinity starts increasing again and at about 185 years reaches 10% (see Figure 10). For the case with a maximum salinity of 7.5% at 2000 m depth, the time until the maximum salinity reaches the repository is about 140 years. For the case with the maximum salinity being initially at 1500 m depth, the brine reaches the repository after about 90 years and the upconed zone is wider than for the other cases (not shown).

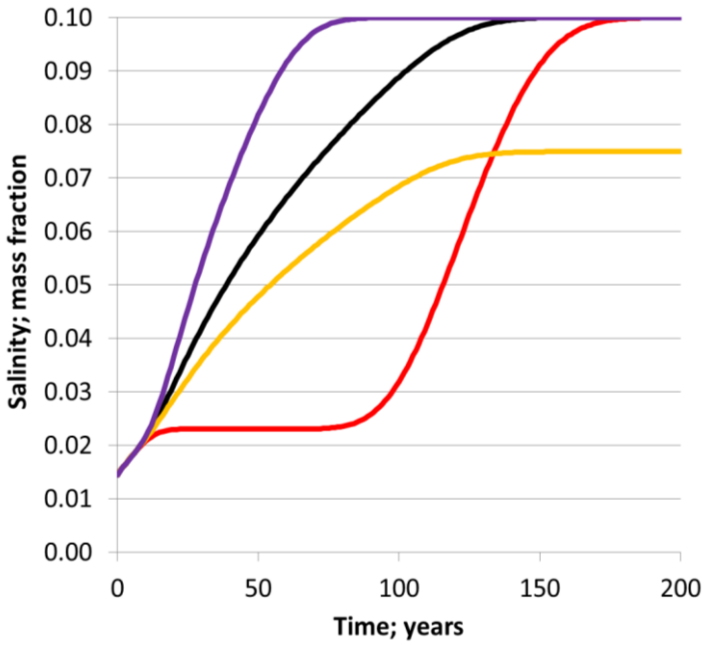


Figure 10: Salinity versus time for the four simulation cases shown in Figure 9 at observation point 6 as defined in Table 3, which lies at the bottom middle of the repository. Initial salinity equal to the Base Case (initial salinity shown in upper left panel in Figure 9; black line), initial salinity constant salinity below 800 m depth being 2.3% (initial salinity shown in upper right panel in Figure 9; red line), initial salinity as for the other cases down to 800 m depth and then increasing linearly to 7.5% at 2000 m depth (initial salinity shown in lower left panel in Figure 9; yellow line), and initial salinity equal to other cases down to 800 m depth and then increasing linearly to 10% at 1500 m depth (initial salinity shown in lower right panel in Figure 9; violet line).

## 5.4 Effect of porosity and permeability

Two of the most important hydraulic parameters of the fracture zones, porosity and permeability, are uncertain. Figure 6 shows that the permeability has a pronounced effect on the saline water intrusion to the repository. The values vary only about 2 orders of magnitude but the result is that either no intrusion of highly saline water occurs at all, or a rather quick intrusion occurs after about 20 years. Simulations based on a range of values of these parameters were run to evaluate the sensitivity of upconing behavior to these controls. The results are shown in Table 5. It is observed in the table that the order of the ratio of porosity to permeability is exactly the same as the order of the breakthrough times. This would be expected for the situation in which there are insignificant density forces, in which groundwater flow is driven only by differences in hydraulic head, because, in Darcy's Law, the ratio (permeability/porosity) is the parameter that multiplies the gradient in hydraulic head when calculating fluid velocity. Thus, irrespective of the partic-

ular boundary conditions, the speed of upconing and timing of salt arrival at the repository depends only on the ratio of porosity and permeability, and not on either parameter independently.

**Table 5: Results with ranks of order of porosity-permeability ratio and of simulated 100g/L salinity breakthrough (in years). All simulations have base-case parameter values except for porosity and permeability.**

| Order (Porosity/ Permeability) | Order breakthrough time | Porosity (-) | Permeability ($m^2$) | (Porosity/ Permeability) ($m^{-2}$) | Time to breakthrough of 100 g/L salinity (years) |
|---|---|---|---|---|---|
| 1 | 1 | $9.00x10^{-04}$ | $1.30x10^{-14}$ | $6.92x10^{+10}$ | 5.0 |
| 2 | 2 | $9.00x10^{-04}$ | $1.30x10^{-15}$ | $6.92x10^{+11}$ | 21.0 |
| 3 | 3 | $1.40x10^{-03}$ | $1.80x10^{-15}$ | $7.78x10^{+11}$ | 25.0 |
| 4 | 4 | $4.00x10^{-04}$ | $1.30x10^{-16}$ | $3.08x10^{+12}$ | 71.0 |
| 5 | 5 | $9.00x10^{-04}$ | $1.30x10^{-16}$ | $6.92x10^{+12}$ | 149.0 |
| 6 | 6 | $4.00x10^{-03}$ | $1.30x^{-16}$ | $3.08x10^{+13}$ | not reached; 0.02 reached at 46 years |
| 7 | 7 | $9.00x10^{-04}$ | $1.30x10^{-17}$ | $6.92x10^{+13}$ | not reached; 0.02 reached at 83 years |
| 8 | 8 | $9.00x10^{-04}$ | $6.70x10^{-18}$ | $1.34x10^{+14}$ | not reached; 0.02 reached at 163 years |

## 5.5 Effect of spatial trends and heterogeneity

The Base Case and the other cases shown above all assume that the deformation zone can be represented in the model by a feature that has a homogeneous permeability and porosity. Clearly, this is a simplifying assumption and therefore, the effect of spatial trends and heterogeneity in the primary hydraulic parameters (permeability and porosity) of the simulated fracture zone is explored in a few simulations.

**DEPTH DEPENDENCE -** The depth dependence of permeability and porosity are calculated by the equations suggested by SKB (Svensson and Follin, 2010). The transmissivity depth dependence is expressed as (eq 2-1 Svensson and Follin, 2010; p. 15):

$$T(y) = T(y = 0)10^{y/k} \qquad (1)$$

in which T is transmissivity ($m^2/s$), $y$ (m) is the depth coordinate (negative below ground) and $k$ (m) is a parameter that expresses the depth interval that yields an order of magnitude difference in transmissivity.

The relation between porosity [1] and transmissivity is defined as:

$$porosity = \frac{\sqrt{0.25\text{s}\ transmissivity}}{borehole\ interval\ length} \quad (2)$$

Inserting equation 2 into equation 1 yields:

$$porosity(y) = \frac{\sqrt{0.25\text{s}\ const\ 10^{y/k}}}{borehole\ interval\ length} \quad (3)$$

with the coefficient 0.25 having the unit (s), *const* ($m^2$/s)being a constant that is determined based on site data. This is obtained by dividing equation 3-2 of Joyce et al. (2010; p. 30) by the borehole interval length [m] observed for the deformation zone to obtain porosity from fracture aperture. Since the permeability ($m^2$) is equal to the transmissivity ($m^2$/s) multiplied by a factor $10^7$ ms divided by the zone thickness (m), the transmissivity value can be replaced by the permeability in the equations. The constant in the porosity equation can be calculated by inserting the values known for a certain depth. In principle, the constant could also be calculated from the transmissivity at depth zero, but in the other modelling cases considered here, the relation between porosity and transmissivity was not used, since both are independently calculated based on measured variables, i.e. transmissivity from borehole tests and the porosity from summing the detected apertures in the zones (as explained previously). For the cases with depth-dependent transmissivity considered here, the value of *k* (in Equation 1) is chosen as 500 m and the resulting *T(0)* = $5.96\text{x}10^{-14}$ $m^2$/s is calculated based on data for zone 725 at a depth of 760 m (see above). For the case with depth-dependent porosity, this yields *const* = 0.34 ($m^2$/s). The depth dependence (Equation 1) is parameterized for the current analysis in a way that gives the same permeability at the depth of measurement (at about 760 m for Zone 725). Below this depth, the permeability is lower and above that it is actually higher than for the base case. For the case in which the porosity is calculated from Equation 3, the porosity is lower below the measured point and higher above.

In Figure 11 results are shown for two cases of spatial trends. Both include depth-dependent permeability and one also includes depth-dependent porosity. It can be seen that upconing occurs much more quickly should both permeability and porosity decrease with increasing depth in the zone. In Figure 12, the breakthrough curves at the mid bottom of the repository are shown for these cases, as well as for the Base Case with constant permeability, with and without depth-dependent porosity according to Equation 3.

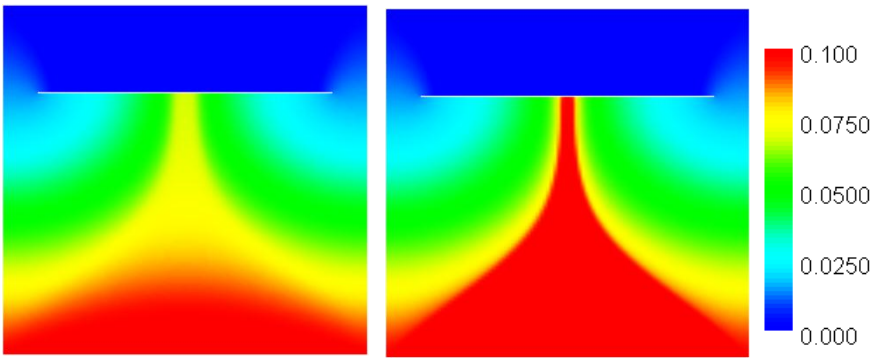


Figure 11: Salinity after 100 years in Base Case model. Left panel case has depth-dependent permeability according to SKB's equation (equation 1) and *k*=500 m and permeability of zone 725 at the measured depth of 760 m. The right panel case has the same depth-dependent permeability and additionally, depth dependent porosity (equation 3). Colors indicate mass fraction of salt, i.e. 0.1 represents 10% salt in the water by weight.

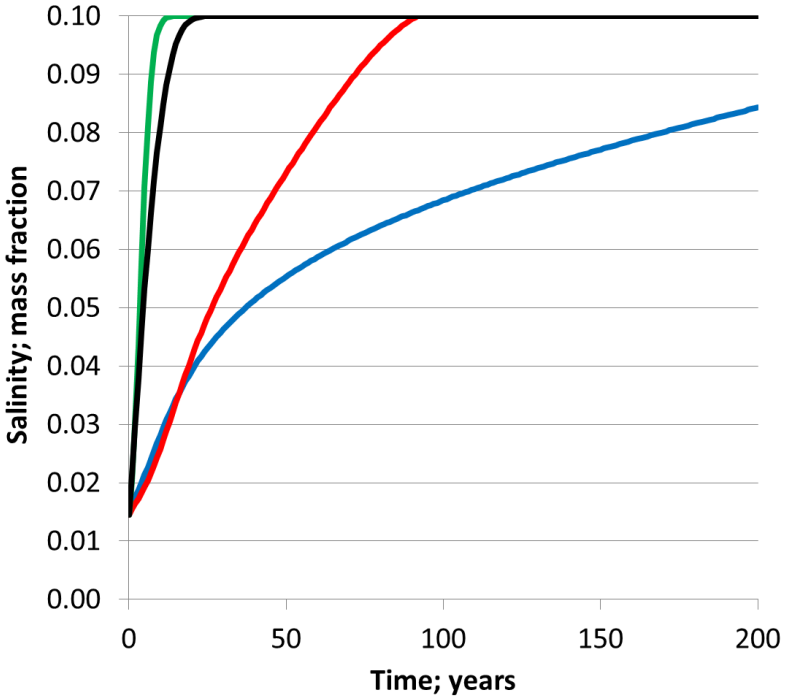


Figure 12: Salinity versus time for the Base Case model and permeability of zone 725 (black line) and the Base Case model with added depth-dependent permeability according to SKB's equation (equation 2) and *k*=500 m and permeability of zone 725 at the measured depth of 760 m (blue line). The red line shows results for the same depth-dependent permeability and additionally, a depth-dependent porosity (equation 3; *const*=0.34 $m^2$/s and *k*=500 m). The green line shows the Base Case model with constant permeability of zone 725 with depth dependent porosity (equation 3; *const*=0.34 $m^2$/s and *k*=500 m).

**HETEROGENEITY -** Arbitrary heterogeneous permeability fields are assumed for the zone, as illustrated in Figure 13. In the first heterogeneous case, heterogeneity in permeability is represented as a pattern of high and low permeability patches via a sine function multiplied by cosine function of $\log_{10}$(permeability). This leads to a span in permeability, *k*, over about 6 orders of magnitude, ($1x10^{-14}$ $m^2$ to $1x10^{-20}$ $m^2$; Equation 4 and Figure 12 with left scale, which shows $-\log_{10}$(permeability)). The distance between adjacent max and min permeability values is about 160 m ($\pi/0.02$ $m^{-1}$) in both x and y directions. This can perhaps roughly represent spatial variability due to fracture aperture and asperity variation within the fracture planes of the zone. The geometric mean of the permeability is taken from the Base Case with permeability of zone 61.

$$k = 6.7 \cdot 10^{-18} \cdot 10^{3 \cdot \sin\left(\frac{0.02\mathrm{m}^{-1}(x-y)}{220}\right) \cdot \cos\left(\frac{0.02\mathrm{m}^{-1}(y-x)}{30}\right)} \qquad (4)$$

In a second heterogeneous case, the heterogeneity in permeability is also represented using the product of a sine function and a cosine function, but one that spans only approximately 2.5 orders of magnitude (equation 5 and Figure 12 with right scale, which shows $-\log_{10}$(permeability)). The spatial distance between max and min permeability values is the same as in the first distribution.

$$k = 1.8 \cdot 10^{-15} \cdot 10^{1.25 \cdot \sin\left(\frac{0.02\mathrm{m}^{-1}(x-y)}{220}\right) \cdot \cos\left(\frac{0.02\mathrm{m}^{-1}(y-x)}{30}\right)} \qquad (5)$$

Porosity is held constant for both heterogeneous fields and other model factors are the same as in the Base Case.

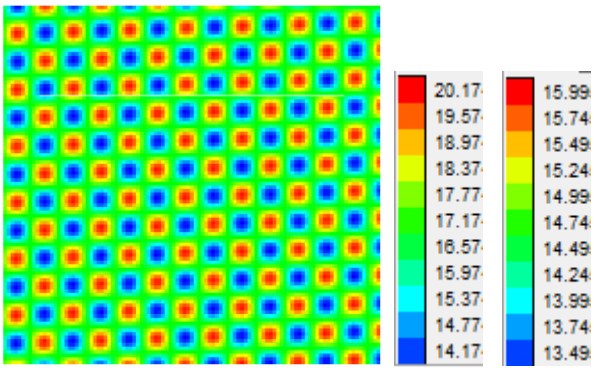


Figure 13: Distribution of permeability in cases with heterogeneity. The coloring expresses $-\log_{10}$(permeability). The left color bar represents the Base Case with permeability of zone 61 (with lower mean and higher variance of permeability) and the right color bar of zone 725 (with higher mean and lower variance of permeability).

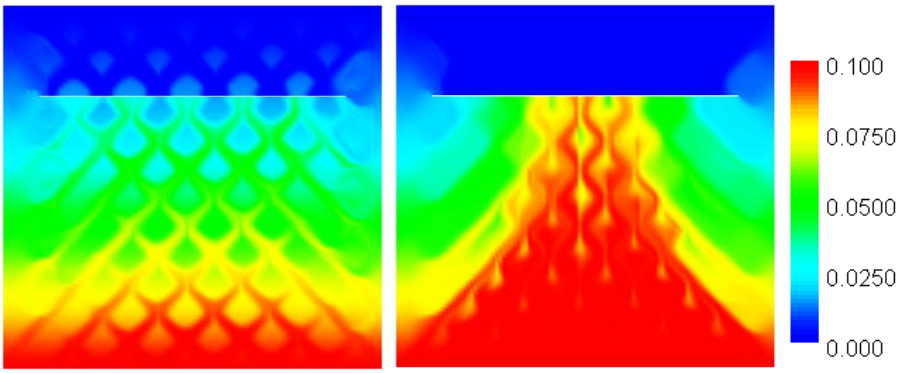


Figure 14: Salinity distributions for heterogeneous permeability patterns. After 200 years for Zone 61 case with lower permeability and higher variance using equation 4 (left panel). Salinity distribution after 10 years and for Zone 725 case with higher permeability and lower variance using equation 5 (right panel). Colors indicate mass fraction of salt, i.e. 0.1 represents 10% salt in the water by weight.

Salinity results from these simulations are shown in Figure 14. In the first heterogeneous case with mean permeability corresponding to Zone 61 and higher permeability variance, no highly saline water reaches the repository at the end of the simulation at 200 years due to the overall lower value of permeability. Upconing occurs preferentially along paths that follow the regions with the greatest permeability. In the lower permeability pockets, the salinity hardly changes at all during the 200 year simulation. For the second heterogeneous case with a mean permeability corresponding to Zone 725, about 2 orders of magnitude higher than the Zone 61 case, and with lower permeability variance, the highly saline water reaches the repository after only 10 years and a steady state is reached at about 35 years. Also in this case the upconing occurs preferentially along paths of high permeability while avoiding patches of low permeability (Figure 14 right panel). Should grouting have been done around the repository tunnels, the intersections of the highest hydraulic conductivity paths would have reduced conductivity, decreasing the connection of the low tunnel pressure to the bedrock and probably reducing the rate of upconing and breakthrough.

## 5.6 Effect of phased tunneling

To see how phased tunneling may influence upconing behavior, a simulation was run in which only a part (100 m of tunnel length) of the entire repository is open at any given time. This was modeled by changing the internal specified pressure boundary condition along repository walls at 30, 60, and 90 years in a way such that different portions of the open repository are represented. Thus three different sections were opened and closed in sequence. This may be considered as representing three phases in repository operation. In reality, the opening and closure of the tunnels will follow a more elabo-

rate pattern, most likely with smaller distances between the tunnel portions that are opened and closed. Figure 15 shows the locations of the open repository sections (small red horizontal bars) and presents the simulated salinity distribution at 30, 40, 60, and 90 years after the first excavation was begun. The results show the situation just before each tunnel section is closed (except at 40 years) and thus the maximum of upconing for each open section. The result for 40 years illustrates how the existing upconed saltwater is held at more or less the same depth even when the water is drawn into a newly opened section.

It can be seen that the upconing through this structure reaches each open section of the repository before each section is closed, with high salinities reaching the open part of the repository.

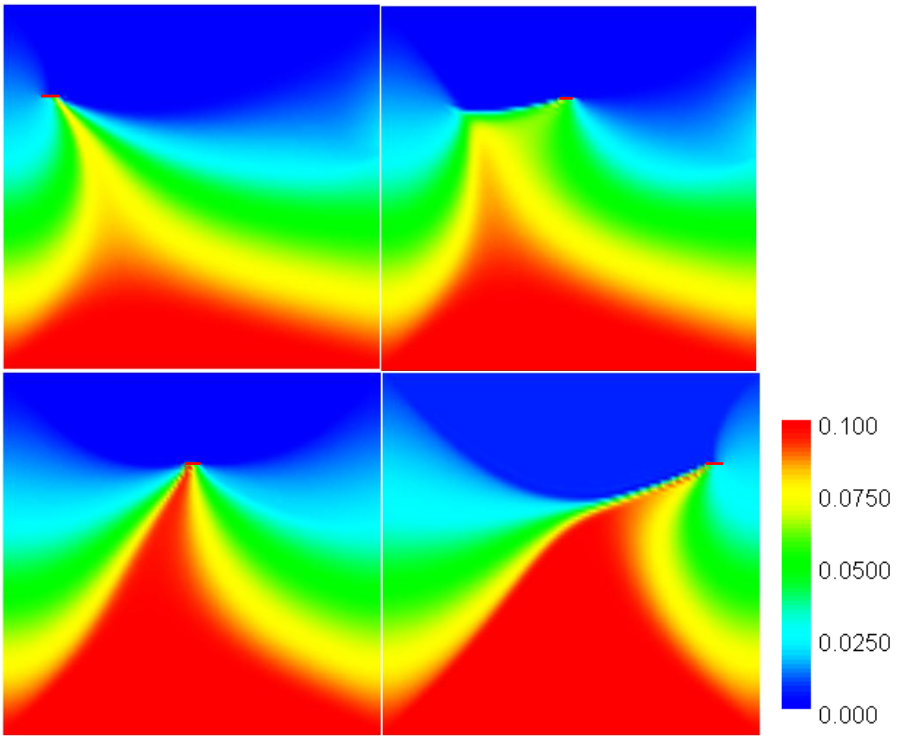


Figure 15: Salinity distribution for a partly open repository with phased tunneling. Permeability is that of Zone 725. The open part of the tunnel is represented by a specified pressure of zero spanning five elements horizontally and two elements vertically, and is thus, 100 m wide and 6 m high. Each section is held open for 30 years. The specified pressure boundary condition locations were changed at 0, 30, 60, and 90 years. Results are shown after 30 years (upper left), 40 years (upper right), 60 years (lower left), and 90 years (lower right). Colors indicate mass fraction of salt, i.e. 0.1 represents 10% salt in the water by weight.

## 5.7 Effect of higher dispersion

The dispersivity values used for most simulations (5. m and 0.1 m for longitudinal and transverse dispersivities, respectively; Table 4) are not well-known values for solute transport in fracture zones and few field measurements have been made at the scales of transport that occur during upconing. Running a simulation with dispersion (i.e., longitudinal and transverse dispersivities) increased by one order of magnitude gives essentially the same breakthrough curves at the bottom center of the repository (not shown). High concentrations are reached at about the same time, but small late-term concentration increases occur, and steady state occurs a few tens of years later than for lower dispersion. Thus, given that the important point is the question if highly salinity water reaches the repository quick enough to adversely impact the resaturation of the buffer, higher dispersivity has negligible impact on the upconing process.

# 6. Discussion of results

**APPROACH -** Because the model is very much a simplification of the real conditions and because values of important physical controlling parameters are to a large extent uncertain, this analysis considers variations of both parameter values and hydrologic conditions, in order to determine important factors that control the upconing behavior at the Forsmark site. Also, this approach defines the range of possible upconing behaviors that might be expected to occur at the site.

**ASSUMPTIONS -** Several key simplifying assumptions that affect the Base Case modelling results were discussed earlier. Three not yet discussed are:

(1) The zone is represented from the surface down to 2000 m as being continuous, at least in view of its permeability and porosity on a scale relative to the discretization of the model domain. This is a basic requirement for the process of upconing to occur; there must be a continuous hydraulic path between the saltwater source and the repository.

(2) A constant pressure boundary condition was employed at the ground surface in this analysis. It is possible that the modeled inflow of water from this boundary might be larger (or smaller) than the net infiltration that is linked to the precipitation at the site. In reality, a situation with recharge less than modeled inflow would lead to water-table drop, which was not modelled. Both a saturated zone extending only part-way to the ground surface and a no-flow boundary at the top of the domain may affect saltwater upconing.

It is possible to evaluate the impact these situations would have on upconing, as follows. Upconing is a simple process primarily controlled by Darcy's Law in the case where the hydraulic gradient imposed by the repository overwhelms the buoyancy forces. In this case, the only factors that control upconing are the pressure (i.e. head) difference between repository and saltwater source zone, the distance to the source of saltwater, and the permeability and porosity of the flowpath that connects the source with the repository. This means that a closed model top (no-flow boundary) will not change the pressure in the repository, so it will not much affect saltwater movement from a source at the bottom of the section. The fact that the repository pressure itself controls the head gradient to any saltwater source makes the controls on upconing clear. It is possible that the saltwater inflow to the top of the tunnel can change when the model top is closed because some saltwater could move upwards around the ends of the tunnel and enter the low-pressure zone above the repository, finally discharging into the top of the repository. However, much less saltwater could enter this way than from

below, so this is expected to be a minor effect. If the top 500 m just above the repository were partly or fully drained, this additional inflow would stop completely, making it even less important.

Further, there are connections to the nearby Baltic Sea in at least some Forsmark boreholes and the upper part of the system has relatively large transmissivity that would enhance connections to shallow water sources. This could lead to recharge of Baltic seawater, in addition to local freshwater recharge, which would limit such a water-table drop, but would deliver brackish water to the repository from above. Such calculations have not been carried out in this study.

The rock, of which the fracture zones are a part, is overlain by Quaternary deposits, which have considerably different hydraulic characteristics and likely greater porosity and thus groundwater storage than the zones. Such deposits are neglected in this study as a specific geologic layer, but these provide a source of water similar to the fixed pressure used in this study, so their effect is already included.

(3) The impacts of variations of some types of conditions within zones that intersect the modeled zone have not been directly considered in this modeling analysis. In the case where the intersecting zones are more transmissive than the one modeled, more upconing could occur in these zones than in the modeled zone, and therefore the salinity at the intersections should also be elevated, forming a changing lateral boundary condition for the zone being modeled. In this particular case, highly saline groundwater could flow toward the excavation from the sides of the modeled region, rather than from the bottom. For this situation, the present approach is conservative, implying lower brine concentrations in the repository than would occur should enhanced upconing occur in transecting structures.

(4) The effects of the heating imposed by the spent nuclear fuel canisters are not accounted for explicitly in the simulations. At repository level the temperature of the rock is expected to increase with max 30 degrees centigrade about 50 years after canister emplacement (SKB, 2011). The larger the distance from the canisters the smaller the heating effect. A 30 degree temperature increase will change the density of the water and its viscosity significantly. The results of this study indicate that it is the change in pressure that mainly drives the upconing and that density effects are not central. Thus the temperature effect on the water density should not change the main results of the study. An increase of 30 degrees centigrade will yield a 50% smaller viscosity, and thus conductivity, around the repository compared to the value used in the modelling. The modeled permeability covers several orders of magnitude and thus this effect should not change the overall conclusions of the study.

(5) In the downconing calculations it is assumed that the repository has no effect on downward flow through the repository. The bentonite should have a lower permeability than the fracture zone modeled, thus in the 2-D model the flow through the repository may be hindered. In 3-D this effect may be less pronounced. In any case, there is a possibility that the downconing could be slowed by the backfilled repository in comparison to the results indicated by the model.

## 6.1 Base case

The three Base Case simulations indicate that, should porosity be constant throughout the vertical fracture zone considered, it is the permeability that has a large influence on the occurrence of intrusion of highly saline water into the repository within 200 years and the timing of this occurrence. The permeability values and the other parameter values for these simulations are derived from the results of SKB's site investigations at Forsmark, and these values are believed to represent the range of conditions that can be encountered at the site. The model results thus indicate that, at parts of the repository that are intersected by relatively high permeability zones, upconing may occur quickly following excavation. In the modeled case with the highest permeability, water with high salt content rises 1500 m to the repository within only two decades after excavating the repository.

In a relatively high-permeability zone, downconing also occurs quickly. The repository fluid freshens due to inflows from above, drawn in by the dropping volume of saline water below the repository. In contrast with upconing, which is driven almost exclusively by hydraulic forces due to the low pressure in excavated tunnels, downconing is driven exclusively by buoyancy forces arising from differences in fluid density.

The rather quick sinking of the upconed saltwater in the high permeability case raises the question of the stability of the assumed initial conditions of the model. Modeling the Base Case with permeability for Zone 725 without a repository, and thus only studying the evolution from the assumed initial conditions, indicates that the salinity field slowly moves downwards (not shown). Thus the initial condition is not at steady state with respect to the boundary conditions applied. A comparison of this simulation with the downconing behavior shown in Figure 5 indicates that the sinking saline cone moves considerably faster than the dropping initial salinity distribution, and thus draws a higher flux of fresh water downwards than does the evolution of the initial conditions. To get a more or less stable (i.e. steady-state) salinity profile that increases with depth, as indicated by field data, the permeability must either be very low (as in the case of Zone 61) or there must be a source of salt, either internally or through transport of salt entering the system through the model boundaries. Alternatively, the current salinity distribution at Forsmark may simply not be in a steady state. The question of

how the initial salinity profile that currently prevails was actually established at Forsmark is not addressed in this study. SKB has discussed this question in their site descriptive modelling of the Forsmark site (SKB, 2008).

## 6.2 Effect of boundaries and topography

The boundary conditions have a significant influence on the simulated migration of saltwater (Figure 7). The lateral model boundaries represent intersections with other fracture zones. Open side boundaries with specified hydrostatic pressure conditions, such as in the Base Case, represent the case of permeable fracture zones that intersect the modeled structure. Assuming closed boundaries at the sides (intersection of the modeled zone with relatively impermeable fracture zones) leads to water input to the open repository exclusively from above and below. This high salinity water is then not diluted by any less-saline water drawn from the lateral model boundaries. However, the closed side boundaries lead to a situation with less total inflow of water to the repository. In effect, the total amount of salt introduced into the repository is smaller for the case with closed boundaries even if the concentration of the water surrounding the repository at late simulation times is considerably higher.

The simulations indicate that the effect of the topography is very small and may be neglected in this type of evaluation. This becomes clear when comparing the large gradients caused by the open repository and the small gradients imposed by the topography.

Given the significant difference in results generated by different boundary conditions, the boundary conditions should be chosen with care. To obtain results that bound a possible span of different responses, several different boundary conditions should be evaluated in any follow-up analysis.

## 6.3 Initial salinity

The initial salinity distribution in the model domain, to a large extent, determines the elapsed time before breakthrough of highly saline water and the maximum concentration when upconing to the repository reaches a steady state. This is not surprising since the water in the fracture zone is discharged into the repository and after enough time has elapsed a steady state solute flux is reached, the configuration of which, in turn, is largely dependent on the boundary conditions. Obviously, the salinity distribution is uncertain at depths greater than have been investigated by measurements. The only way to explore the effects of the range of possible different pre-existing salinity distributions is to simulate them.

The impact of the initial salinity distribution of waters that are below the repository at different depths depends on the transmissivity of the zone be-

low the repository. If the transmissivity is relatively small, the inflows become small and the uncertainties in the results caused by the initial salinity distribution diminish, since only the well-characterized waters near the repository can reach the repository before closure within 200 years.

## 6.4 Permeability and porosity

As discussed previously, with a fixed set of boundary conditions, a difference of only two and a half orders of magnitude of the modeled permeability value causes there to be either (1) no saline water intrusion at all or (2) significant upconing of highly saline waters to the repository within only decades. Considering the uncertainties in the determination of the transmissivity (and thus permeability) of the zones, permeability (or transmissivity) is judged to be a key parameter for determining the likelihood of the occurrence of significant upconing.

However, the porosity also has a strong influence on the simulated upconing. The porosity does not affect the pressure field or the Darcy velocity, but the velocity of the water resulting from a given Darcy velocity is inversely proportional to the porosity, and thus the speed of upward transport of salt depends on the porosity.

The porosity of a zone and its transmissivity are likely to be closely correlated. The worst case, causing upconing to occur most quickly, is the case of high transmissivity and low porosity. This may not be very likely, considering that the values are correlated and higher transmissivity is usually associated with higher porosity. Assuming a strict correlation between transmissivity and porosity (for instance by using equation 2) may, however, not capture the entire span in the uncertainty relating to the upconing behavior of the system. Given the uncertainty in the permeability and porosity, an adequate range needs to be evaluated to be able to assess the likelihood of upconing occurring and its speed.

The ranking of porosity divided by permeability (Table 5) shows that this ratio is perfectly correlated to the time to breakthrough of highly saline water into the repository. Thus the single key parameter controlling speed of upconing is the ratio of permeability to porosity.

## 6.5 Density forces

To explain that the ratio of permeability to porosity is the key parameter controlling upconing speed, Darcy's Law may be considered, noting that this is exactly the parameter in Darcy's Law that controls velocity in a fluid of constant density. This indicates that flow driven by the large gradients created by the excavation is decisive for the salt transport and that the variable density only plays a secondary role during upconing. In contrast, for

downconing, density forces are the dominant ones. A simulation with Base Case parameters that assumed no dependence of the density on the salt content of the water shows that the salinity pattern and breakthrough time of highly saline water are similar. The breakthrough of highly saline water is delayed about 40 years compared to the Base Case with density dependent transport (all other factors kept constant). This result is in agreement with findings of Werner et al. (2009) who concluded that the influence of density is minor relative to the combined influence of the pumping rate and the distance from the wellbore to the initial interface, in their experimental tank upconing experiments.

## 6.6 Spatial trends and heterogeneity

Spatial trends in controlling parameters, particularly depth-dependent permeability, influence the upconing behavior significantly. Comparison of the left panel of Figure 5 with the left panel of Figure 11 illustrates typical differences that may be expected. In the case with decreasing permeability with depth (Figure 11 left panel), the upconed saltwater body is narrower since more water is drawn from the boundaries at depths below the repository above the bottom boundary. Moreover, the time to breakthrough of highly saline water is delayed from about ten years to about 200 years. Upconing becomes slower with the depth-dependent permeability (Figure 12, compare blue and black lines).

Permeability and porosity are likely to be correlated. It was assumed for simplicity that a perfect correlation exists between the two. A porosity decreasing with depth and depth-dependent permeability were thus implemented together. Depth-dependent porosity does not influence the salinity distribution at steady state, as expected. However, the time for breakthrough of highly saline water at the repository is strongly affected and occurs around 100 years. This result lies between the case of no depth dependence of permeability and porosity and the case of depth-dependent permeability with constant porosity. The case with constant permeability and decreasing porosity with depth results in even faster breakthrough of highly saline waters at the repository. This case may not be very likely, but it provides a bound to the range of possible breakthrough times.

In terms of the timing of the arrival of highly saline water into the modeled repository, the assumption of depth-dependent permeability and porosity provides a possible range of arrival times from a rather quick breakthrough between only ten and 100 years following excavation, and at most to a long-enough extreme delay such that breakthrough would not occur at all, since the facility can be expected to be backfilled before 200 years.

The simulations with heterogeneity in permeability, modeled as sinusoidal spatial functions, result in clearly different spatial salinity patterns during upconing from the respective homogeneous cases (Figure 14). However, in terms of time to breakthrough of highly saline water, the difference is not large, in comparison with the respective homogeneous cases. Grouting would lower the conductivity in the highest conductivity zones. However, because heterogeneity does not significantly affect the overall upconing response in comparison with the homogeneous case, the effect of grouting in the heterogeneous case was not analysed. These results are dependent on the type of spatial permeability distribution assumed. The spatial distributions according to equations 4 and 5 yield fields with continuous permeability close to the values of respective homogeneous case that are surrounded by low and high permeability pockets. A comparison of the two heterogeneous cases indicates that the upconing occurs along paths through the regions with the greatest permeability. It may be interesting to investigate how different spatial arrangements of the spatial permeability field influence the results. An evaluation of different possible spatial permeability fields is, however, beyond the scope of the present study.

## 6.7 Phased tunneling

The model cases simulating phased tunneling show that in a situation with permeability representing zone 725, the upconed saltwater body approaches the open tunnel section from below but the highly saline water does not reach the open section as quickly as in the respective case with an entirely open repository (compare Figure 5 with Figure 15 upper left panel). When the first section is closed and the second is opened after 30 years, the upconed saltwater moves laterally (see Figure 15 upper left panel) towards the newly opened section. After 60 years the highly saline water has reached the open repository section. When the last section is opened it takes about 30 years for the upconed saltwater to reach it.

Locally, phased tunneling may produce stronger upconing in terms of higher salt concentration than the case in which the entire repository is all open at once. It is notable that the ends of the completely open repository do not receive highly saline waters due to the shape of the flow field created when the entire repository is opened (Figure 5) and due to their proximity to fresher water within intersecting fracture zones at the lateral boundaries. In contrast, Figure 15 shows that upconing in which highly saline waters reach the repository may occur after only some decades at the far end of the partial repository section that is open, and for a given location, the phased tunnelling yields higher concentrations. Thus, to make more realistic predictions of the upconing in a sequentially opened tunnel, the sequence of opening and closure of different parts of the tunnels may have to be represented with more detail.

## 6.8 Tunnel resaturation

Figure 5 shows that downconing and complete refreshening of the groundwater surrounding the repository can occur quickly, within a few tens of years following closure with full resaturation of the repository. However, this simulation assumes that the repository tunnels are immediately resaturated at the moment the repository is backfilled and closed. In reality, resaturation is expected to be a slow process (lasting from perhaps hundreds to thousands of years; Åkesson et al., 2010, Figure 2‑35) due to the low permeability of the host rock. As long as the repository remains unsaturated, water pressure in the tunnels will remain near-atmospheric and a strong hydraulic gradient will drive groundwater flow and upconing toward the tunnels, as it does for conditions during excavation. Thus, although downconing would freshen repository groundwaters once it begins, downconing would begin only once the repository water pressure increases to near-hydrostatic conditions, and this occurs only when the tunnels become almost fully resaturated. The implication is that upconed brine would remain in the vicinity of the bentonite clay barriers for almost as long as the repository takes to fully resaturate, increasing the reasons for concern about impacts of upconed brine on bentonite swelling and thus, on the planned functioning of the bentonite barrier. If particular sections of the repository tunnels are resaturated sooner or later, this would imply, respectively, that groundwater in some sections of the repository could become fresh sooner or could remain salty longer.

# 7. Conclusions

The upconing of saltwater from below a repository for spent nuclear fuel and its subsequent intrusion is evaluated in this study via numerical modeling. The objective is to increase the understanding of which configurations and parameters control the upconing behavior and to assess whether this process may be likely to occur in a repository at Forsmark, Sweden.

**MAIN CONCLUSION –**The results of this simulation analysis show that upconing behavior is strongly affected by the ratio of permeability to porosity in any zone in which upconing might occur. Within the full range of parameters that are likely to occur at the Forsmark site, the model yields either no significant upconing at all during the operational period of the repository or intrusion of brine-type waters after only one to a few decades.

Upconing of saltwater can, on the basis of this study, not be ruled out as a significant process to consider for the repository at Forsmark. This assessment is in line with the assessment of SKB that the possibility for upconing of deep saline groundwater in steeply dipping zones of high transmissivity is

considered to be one of the main hydrogeological uncertainties in the site descriptive modelling SKB (2008; p. 233).

**CONTROLS ON UPCONING –** Upconing is mainly driven by the pressure differences due to the excavated repository and not much by the effects of the variable density of the water. In contrast, the downconing of the saltwater after repository closure is solely driven by variable-density forces.

For each fracture zone intersecting the repository, upconing is controlled by several factors. The initial salt distribution and hydraulic conditions significantly impact the upconing process within any given fracture zone. For the fracture zone itself, low permeability leads to little upconing so that the water intruding the repository during the excavated period consists of the water initially surrounding the repository. The salt content of this water is determined by the initial conditions. In contrast, high permeability may lead to intrusion of highly saline water into the repository with a source at some distance away from the repository, for example located one kilometer below the tunnels. The timing of breakthrough to the repository and evolution of concentration of intruding saltwater in a particular fracture zone depends in part on the conditions of its intersecting neighbor zones. For a situation in which there is no water inflow to the zone from below, increased permeability leads to increased inflow from intersecting fracture zones. For high permeability values this may imply that saline water may not be drawn into the repository, if salinities are low in shallow portions of intersecting zones which would be the primary sources of water entering the repository in this case. However, the groundwater salinity in the intersecting fracture zones may change with time due to upconing or saltwater redistribution in those zones, and eventually the laterally intruding water from shallow depths in intersecting zones may contribute higher salinities to the repository.

Some types of heterogeneity within fracture zones will not strongly affect the occurrence of upconing. The properties of continuous paths connecting the highest permeabilities within a heterogeneous fracture zone control the occurrence of upconing.

Phased tunneling influences upconing behavior, but because the saline water body moves laterally from a newly-closed section to a newly-open section, the occurrence of upconing is not inhibited by phased tunneling. In contrast, the salt content of the intruding water may be greater in segments of a partially open repository than it would be for a repository that is completely open, due to the greater distance of each segment from intersecting fracture zones that would contribute relatively fresh water to repository inflow.

**RELEVANCE TO FORSMARK SITE –** The actual values of parameters that control the upconing behavior for a Forsmark repository are uncertain.

This is true for the permeability and porosity of the zones but also for the initial salinity distribution. In particular there are no data on permeability, porosity or salinity below 900 m at Forsmark. Therefore the effects of this uncertainty need to be evaluated to be able to make adequate predictions. A relatively simple conceptual model like the one used in this study is helpful in defining the modes of upconing behavior that are possible, and in defining the factors controlling this process. More elaborate structural models could be used to check more carefully which of the range of conditions that are here found to be plausible for the Forsmark site are most applicable.

The primary result here is that significant upconing and brine intrusion into a Forsmark repository may possibly occur within only a few tens of years of the beginning of excavation and saltwater can remain in a repository section until full resaturation has occurred in that section. Thus, saltwater may reside within the repository for as long as it takes to resaturate. This may be an extended period following closure due to the low-permeability host rock and the long-term presence of saltwater may adversely impact swelling of some bentonite barriers.

# 8. References

Berg, C., Levén, J., and Nilsson A.-C., 2005. Hydrochemical logging in KFM07A. Forsmark site investigation, SKB P-05-187, Swedish Nuclear Waste Management Co, Stockholm.

Follin, S., Levén J., Hartley L., Jackson P., Joyce S., Roberts D., and Swift B., 2007. Hydrogeological characterisation and modelling of deformation zones and fracture domains, Forsmark modelling stage 2.2, SKB R-07-48, Swedish Nuclear Waste Management Co, Stockholm.

Florberger, J., Hjerne, C., Ludvigson, J.-E., and Walger, E., 2006. Single-hole injection tests in borehole KFM01D. Forsmark site investigation, SKB P-06-195, Swedish Nuclear Waste Management Co, Stockholm.

Forssman, I., Zetterlund, M., Forsmark, T., and Rhén, I., 2006. Correlation of Posiva Flow Log anomalies to core mapped features in KFM06A and KFM07A. Forsmark site investigation, SKB P-06-56, Swedish Nuclear Waste Management Co, Stockholm.

Hjerne, C., Ludvigson, J.-E., and Lindquist, A., 2005. Single-hole injection tests in boreholes KFM06A and KFM06B. Forsmark site investigation, SKB P-05-165, Swedish Nuclear Waste Management Co, Stockholm.

Joyce, S., Simpson, T., Hartley, L., Applegate, D., Hoek, J., Jackson, P., Swan, D., Marsic, N., Follin, S., 2010, Groundwater flow modelling of periods with temperature climate conditions – Forsmark, SKB R-09-20, Swedish Nuclear Waste Management Co, Stockholm.

Karnland, O., Muurinen, A., and Karlsson, F., 2005. Bentonite swelling pressure in NaCl solutions-experimentally determined data and model calculations. in Alonso and Ledesma (eds.) *Advances in Understanding Engineered Clay Barriers*, Taylor and Francis Group, London, p. 241-256.

Laaksoharju, M., Andersson, C., Tullborg, E.-L., Wallin, B., Ekwall, K., Pedersen, K., and Nilsson, A.-C., 1999. Re-sampling of the KLX02 deep borehole at Laxemar, SKB R-99-09, Swedish Nuclear Waste Management Co, Stockholm.

Nilsson, K., 2006. Hydrochemical logging in KFM09A. Forsmark site investigation, SKB P-06-95, Swedish Nuclear Waste Management Co, Stockholm.

Petersson, J., Skogsmo, G., Berglund, J., Wängnerud, A., and Stråhle, A., 2005. Boremap mapping of telescopic drilled borehole KFM06A and core

drilled borehole KFM06B. Forsmark site investigation, SKB P-05-101, Swedish Nuclear Waste Management Co, Stockholm.

Petersson, J., Skogsmo, G., von Dalwigk, I., Wängnerud, A., and Berglund, J., 2006. Boremap mapping of telescopic drilled borehole KFM01D. Forsmark site investigation, SKB P-06-132, Swedish Nuclear Waste Management Co, Stockholm.

Pitkänen, P., Partamies, S., Lahdenperä, A.-M., Ahokas, T., and Lamminmäki, T., 2009. Results of monitoring at Olkiluoto in 2008, hydrogeochemistry, Posiva Working Report 2009-44, Posiva Oy, Eurajoki.

Prieto, C., Kotronarou, A., and Destouni, G., 2006.The influence of temporal hydrological randomness on seawater intrusion in coastal aquifers, *Journal of Hydrology*, Vol. 330, p. 285-300.

Reilly, T.E., and Goodman, A.S., 1987. Analysis of saltwater upconing beneath a pumping well, *Journal of Hydrology*, Vol. 89, 169-204.

Rubin, Y., 2003. *Applied stochastic hydrogeology*, Oxford University Press, New York.

SKB, 2008. Site description of Forsmark at completion of the site investigation phase, SDM-Site Forsmark, SKB TR-08-05, Swedish Nuclear Waste Management Co, Stockholm.

SKB, 2009. Underground design Forsmark, Layout D2, SKB R-08-116, Swedish Nuclear Waste Management Co, Stockholm.

SKB, 2011. Long-term safety for the final repository for spent nuclear fuel at Forsmark, main report of the SR-Site project, SKB TR-11-01, Swedish Nuclear Waste Management Co, Stockholm.

Stephens, M. B., Fox, A., La Pointe, P., Simeonov, A., Isaksson, H., Hermanson, J., and Öhman, J., 2007. Geology Forsmark. Site descriptive modelling Forsmark stage 2.2, SKB R-07-45, Swedish Nuclear Waste Management Co, Stockholm.

Smellie J., Tullborg, E.-L., Nilsson, A.-C., Sandström, B., Waber, N., Gimeno, M., and Gascoyne, M., 2008. Explorative analysis of major components and isotopes. SDM-Site Forsmark, SKB R-08-84, Swedish Nuclear Waste Management Co, Stockholm.

Svensson, U., 2006. The Forsmark repository, modelling changes in the flow, pressure and salinity fields, due to a repository for spent nuclear fuel, SKB R-05-57, Swedish Nuclear Waste Management Co, Stockholm.

Svensson, U., and Follin, S., 2010. Groundwater flow modelling of the excavation and operation phases – SR-Site Forsmark, SKB R-09-19, Swedish Nuclear Waste Management Co, Stockholm.

Teurneau B., Forsmark, T., Forssman, I., Rhén, I., and Zinn, E., 2008. Correlation of Posiva Flow Log anomalies to core mapped features in KFM01D, KFM07C, KFM08A, KFM08C and KFM10A. Forsmark site investigation, SKB P-07-127, Swedish Nuclear Waste Management Co, Stockholm.

Väisäsvaara, J., Leppänen, H., and Pekkanen, J., 2006. Difference flow logging in borehole KFM01D. Forsmark site investigation, SKB P-06-161, Swedish Nuclear Waste Management Co, Stockholm.

Voss, C.I., and Provost, A.M., 2002. SUTRA: A model for saturated-unsaturated, variable-density ground-water flow with solute or energy transport, Water-Resources Investigation Report 02-4231. US Geological Survey, Reston, Virginia, USA.

Werner, A. D., Jakovovic, D., and Simmons, C.T., 2009. Experimental observations of saltwater up-coning, *Journal of Hydrology* Vol. 373, p. 230–241.

Åkesson, M., Kristensson, O., Börgesson, L., Dueck, A., and Hernelind, J., 2010. THM modelling of buffer, backfill and other system components. Critical processes and scenarios, SKB TR-10-11, Swedish Nuclear Waste Management Co, Stockholm.

2013:28

The Swedish Radiation Safety Authority has a comprehensive responsibility to ensure that society is safe from the effects of radiation. The Authority works to achieve radiation safety in a number of areas: nuclear power, medical care as well as commercial products and services. The Authority also works to achieve protection from natural radiation and to increase the level of radiation safety internationally.

The Swedish Radiation Safety Authority works proactively and preventively to protect people and the environment from the harmful effects of radiation, now and in the future. The Authority issues regulations and supervises compliance, while also supporting research, providing training and information, and issuing advice. Often, activities involving radiation require licences issued by the Authority. The Swedish Radiation Safety Authority maintains emergency preparedness around the clock with the aim of limiting the aftermath of radiation accidents and the unintentional spreading of radioactive substances. The Authority participates in international co-operation in order to promote radiation safety and finances projects aiming to raise the level of radiation safety in certain Eastern European countries.

The Authority reports to the Ministry of the Environment and has around 270 employees with competencies in the fields of engineering, natural and behavioural sciences, law, economics and communications. We have received quality, environmental and working environment certification.

**Strålsäkerhetsmyndigheten**
**Swedish Radiation Safety Authority**

SE-171 16 Stockholm
Solna strandväg 96

**Tel:** +46 8 799 40 00
**Fax:** +46 8 799 40 10

**E-mail:** registrator@ssm.se
**Web:** stralsakerhetsmyndigheten.se